

DOE/RF/00646--71

RESEARCH TRIANGLE INSTITUTE



November 1994

**WIND TUNNEL EVALUATION OF THE RAAMP SAMPLER**

**Work Assignment Number: II-238**

**FINAL REPORT**

**RTI Work Assignment Leader: R.W. Vanderpool  
Research Triangle Institute  
Research Triangle Park, NC 27709**

**EPA Contract No. 68D10009**

**Project Officer: Roosevelt Rollins  
Atmospheric Research and Exposure Assessment Laboratory  
Methods Research and Development Division  
Source Methods Research Branch**

**Task Manager: Fu-Lin Chen  
Atmospheric Research and Exposure Assessment Laboratory  
Methods Research and Development Division**

**U.S. Environmental Protection Agency  
Research Triangle Park, NC 27711**

**MASTER**

Post Office Box 12194    Research Triangle Park, North Carolina 27709-2194  
Telephone: 919 541-6000    FAX: 919 541-5985

**DISTRIBUTION OF THIS DOCUMENT IS UNLIMITED**

# WIND TUNNEL EVALUATION OF THE RAAMP SAMPLER

Work Assignment Number: II-238

## FINAL REPORT

Prepared for:

Fu-Lin Chen  
Aerosol Physics and Methods Branch  
Methods Research and Exposure Assessment Laboratory  
U.S. Environmental Protection Agency  
Research Triangle Park, NC 27711

Prepared by:  
Robert W. Vanderpool  
Thomas M. Peters  
Center for Environmental Technology  
Research Triangle Institute  
Research Triangle Park, NC 27709

RTI Work Assignment Leader:



RTI Project Manager:



U.S. EPA Work Assignment Manager:



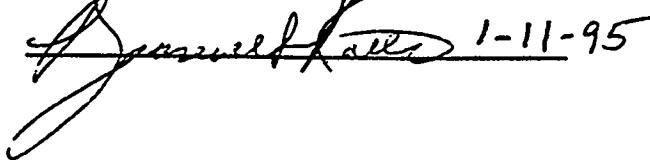
U.S. EPA Section Chief:



U.S. EPA Branch Chief:



U.S. EPA Project Officer:

 1-11-95

## **WIND TUNNEL EVALUATION OF THE RAAMP SAMPLER**

**Prepared by:**

**Robert W. Vanderpool  
Thomas M. Peters**

**Research Triangle Institute  
Center for Environmental Technology  
P.O. Box 12194  
Research Triangle Park, NC 27709**

**Prepared for:**

**U.S. Environmental Protection Agency  
Atmospheric Research and Exposure Assessment Laboratory  
Research Triangle Park, NC 27711  
EPA Contract No. 68D10009  
RTI Project No. 91U-6960-238**

**Project Officer  
Roosevelt Rollins**

**November 1994**

### **DISCLAIMER**

This report was prepared as an account of work sponsored by an agency of the United States Government. Neither the United States Government nor any agency thereof, nor any of their employees, makes any warranty, express or implied, or assumes any legal liability or responsibility for the accuracy, completeness, or usefulness of any information, apparatus, product, or process disclosed, or represents that its use would not infringe privately owned rights. Reference herein to any specific commercial product, process, or service by trade name, trademark, manufacturer, or otherwise does not necessarily constitute or imply its endorsement, recommendation, or favoring by the United States Government or any agency thereof. The views and opinions of authors expressed herein do not necessarily state or reflect those of the United States Government or any agency thereof.

## ABSTRACT

Wind tunnel tests of the Department of Energy RAAMP (Radioactive Atmospheric Aerosol Monitoring Program) monitor have been conducted at wind speeds of 2 km/hr and 24 km/hr. The RAAMP sampler was developed based on three specific performance objectives: 1) Meet EPA PM10 performance criteria, 2) Representatively sample and retain particles larger than 10  $\mu\text{m}$  for later isotopic analysis, 3) Be capable of continuous, unattended operation for time periods up to two months. In this first phase of the evaluation, wind tunnel tests were performed to evaluate the sampler as a potential candidate for EPA PM10 reference or equivalency status.

As an integral part of the project, the EPA wind tunnel facility was fully characterized at wind speeds of 2 km/hr and 24 km/hr in conjunction with liquid test aerosols of 10  $\mu\text{m}$  aerodynamic diameter. Results showed that the facility and its operating protocols met or exceeded all 40 CFR Part 53 acceptance criteria regarding PM10 size-selective performance evaluation. Analytical procedures for quantitation of collected mass deposits also met 40 CFR Part 53 criteria. Modifications were made to the tunnel's test section to accommodate the large dimensions of the RAAMP sampler's instrument case.

Performance tests conducted under still air conditions indicated that the internal size fractionating components of the sampler were performing approximately as intended with a measured average stage penetration value close to 50% for 10  $\mu\text{m}$  aerodynamic diameter aerosols. Wind tunnel tests using 10  $\mu\text{m}$  liquid aerosols, however, provided early indications that the RAAMP sampler was not a likely candidate for submission for PM10 reference or equivalency status. For this particle size of the greatest interest, the sampler's effectiveness was measured to be 29% and 14% at wind speeds of 2 km/hr and 24 km/hr, respectively. Extensive mass balance tests showed that particle losses to the sampler's inlet screen, impactor stage, and other internal components were excessive. For example, fractional particle losses to the sampler's inlet screen were measured to be approximately 40% at a wind speed of 24 km/hr. Fractional losses to the impactor stage were measured to be approximately 25% independent of wind speed. The size and close proximity of the RAAMP sampler's instrument case to the sampling inlet were also found to adversely affect the aspiration characteristics of the inlet.

During the course of the project, some component modifications were made by the RAAMP sampler's manufacturer. These component changes included redesign of the inlet, transport tube, transition section, and impactor stage. The effect of these component modifications was evaluated in the wind tunnel. Results showed that none of these design changes reduced the sampler's dependence on wind speed nor significantly reduced internal particle losses. Recommendations were made regarding future development of the RAAMP program.

## 1.0 INTRODUCTION

In recognition of the size-selective nature of the human respiratory system to airborne particulates, the Environmental Protection Agency (EPA) proposed revisions in 1984 to the National Ambient Air Quality Standards (NAAQS) for particulate matter. As later promulgated, new primary standards were established for particulate matter representing the presumed respirable fraction (PM<sub>10</sub>). Accompanying the new standard was a new Federal Reference Method for the determination of PM<sub>10</sub> in the atmosphere and provisions for the designation of reference and equivalent sampling methods.

The Department of Energy (DOE) requires continuous long-term ambient sampling to determine radioactive particle concentrations in the atmosphere. In anticipation that the EPA (in conjunction with DOE) would ultimately require PM<sub>10</sub> surveillance for respirable radioactive aerosols, the RAAMP (Radioactive Atmospheric Aerosol Monitoring Program) monitor was developed. Unlike commercially available size-selective monitors, the RAAMP monitor was developed to provide continuous operation for extended time periods. The sampler was also designed to retain particles larger than the respirable size for later quantitation of particle-borne isotopes.

Because wind tunnel evaluation of a candidate PM<sub>10</sub> monitor is necessary to ensure that the monitor meets EPA PM<sub>10</sub> performance criteria, an Interagency Agreement (RW89936948-01-0) was established between DOE and EPA's Atmospheric Research and Exposure Laboratory (AREAL) to evaluate the RAAMP sampler. Based upon initial wind tunnel test results, the sampler's size-selective components may be redesigned, fabricated, and performance tested until an acceptable design is achieved. Per terms of the Interagency Agreement, three separate phases were to be conducted with Phase 1 including initial evaluation of the sampler, Phase 2 involving any necessary redesign and evaluation of system components, and Phase 3 including final wind tunnel evaluation and reporting.

This report summarizes work accomplished during Phase 1 of the Agreement between DOE and EPA-AREAL. Specific tasks conducted during this phase included initial system checkout and flow calibration tests, size selective tests performed under static conditions, and wind tunnel evaluation of the sampler versus wind speed. Limited tests were also conducted to evaluate changes made to the sampler design during the course of this project. This report includes a description of the wind tunnel facility, a summary of test procedures used during the evaluation, and a summary of test results.

## 2.0 WIND TUNNEL CHARACTERIZATION

### 2.1 WIND TUNNEL DESCRIPTION

To evaluate candidate size-selective samplers, a wind tunnel is required to provide a controlled environment having well defined velocity profiles and monodisperse particle concentrations. An overview of the EPA-AREAL Aerosol Test Facility and the wind tunnel is presented in Figure 1. In plan view, the wind tunnel is rectangular in shape with outside dimensions being approximately 4.9 m by 18.1 m. Flow through the recirculating wind tunnel during all operations is counter-clockwise. There are few flow obstructions and a number of doors allow access to all sections of the wind tunnel for cleaning. At the test section the wind tunnel cross-section is 1.52 m (5 ft) wide by 1.22 m (4 ft) high.

Wind tunnel performance specifications outlined in 40 CFR Part 53 require that sampler performance tests be conducted at speeds of 2, 8, and 24 km/hr. Since the EPA-AREAL wind tunnel is of fixed geometry, varying wind speeds are achieved by controlling the volumetric flowrate. Major flow through the wind tunnel is provided by a Twin City centrifugal plenum fan capable of providing approximately 1,540 m<sup>3</sup>/min (54,400 cfm) against 0.75 kPa (3 inches of water) pressure drop at 709 rpm at a power requirement of 29 kW (39 hp). This blower is capable of driving the wind tunnel at speeds up to 48 km/hr (30 mph). Wind speed is controlled through an eddy-clutch speed control system which regulates the rotational rate of the fan. Because high speed operation of the wind tunnel adds a significant amount of heat to the recirculating airstream, a bypass chiller/blower system is used to control the tunnel temperature. Controlled circulation of chilled (approximately 5° C) water through cooling vanes in the chiller counteracts the continued heat input and allows the wind tunnel to be operated at near ambient temperature conditions.

Because low rotational fan speeds cannot be reliably maintained for long time periods, a windspeed of 2 km/hr in the test section cannot be achieved simply by reducing the speed of the large blower. The desired 2 km/hr operating condition can be achieved, however, by bypassing the larger blower (using a large damper) and operating the filter/chiller at reduced flow of 57 m<sup>3</sup>/min using a series of dampeners upstream and downstream of the bypass blower.

Prior to conducting the RAAMP sampler performance evaluation, all internal surfaces of the wind tunnel were thoroughly cleaned to remove aerosol deposits collected during several months of prior wind tunnel operation. The wind tunnel was also modified at this time to include a bank of medium efficiency bag-type filters downstream of the test section (Figure 1) to remove aerosols not collected by the samplers. Filters of this type were also present in the bypass/chiller section of the wind tunnel. These primary filter banks effectively prevented the continuous accumulation of material on the

large blower, chiller coils, and chiller fan and dramatically reduced the background level of the fluorescent material in the airstream. Minimizing recirculation of aerosols also resulted in a near steady-state aerosol concentration during the day with measured concentrations never deviating more than 5% from the mean.

## 2.2 VELOCITY UNIFORMITY

Performance specifications outlined in 40 CFR Part 53 require that the velocity profile in the test section be well characterized at each of the three wind speeds and meet specific acceptance criteria. Wind speed and turbulence intensity must be measured by hot-wire anemometry at a minimum of 12 points in a cross-sectional area of the test section. The wind tunnel meets velocity acceptance criteria if the mean wind speed in the test section is within 10% of the desired mean and the variation at any test point in the test section does not exceed 10% of the measured mean.

A constant temperature anemometer (CTA) system was used to measure the mean velocity, root mean square (RMS) velocity, and turbulence intensity at various traverse positions in the test section of the wind tunnel. The CTA system consisted of the following hardware components: 1) Mainframe (Dantec Model# 56B01, Serial# 121), 2) Bridge (Dantec Model# 56C01), 3) Bridge plug-in unit (Dantec Model# 56C17), 4) Voltmeter (TSI Model# 1076), and 5) Flow Probe (Dantec Model# 55R01, Serial# FF#1). A Gateway 486/33 computer equipped with a Metrabyte analog to digital converter board (Metrabyte, Model# DAS-16) and a Dantec Acquire data acquisition software system was used to sample the tunnel velocity at a user-selectable frequency and number of data points. The number of data collected for each traverse position was set at 4096.

The CTA system was first calibrated for velocities ranging from 0.5 km/hr to 40 km/hr using a flow calibrator (TSI Model# 1125, Serial# 358K). The probe of the CTA system was then inserted through the sampling ports in the test section and the sampling frequency (inverse of the sampling integration time) was optimized to measure all of the RMS component for each wind speed. A full traverse of the tunnel was conducted by manually moving the CTA flow probe and sampling the velocity at each traverse position.

Figure 2 depicts the location of the 15 traverse points used for the velocity characterization. Due to logistical constraints, these equally-spaced points could not be placed in the same vertical plane as that used for the aerosol sampling but were in plane located approximately 1 m downstream. Comparison tests showed that no appreciable variation in velocity profile existed over this 1 m longitudinal distance in the test section.

Experience has shown that the desired mean wind tunnel velocity in the test section can be achieved relatively easily and that variations in mean velocity are minimal throughout the day. However, velocity profile measurements in the test section at a

mean wind speed of 2 km/hr have shown that a uniform velocity profile in the test section can only be achieved at this wind speed by altering the flow field upstream of the test section. In the EPA-AREAL facility this flow modification was conducted at a point approximately 8 m upstream of the test section. Figure 3 depicts the configuration of the plywood baffle required to flatten the velocity profile at a wind speed of 2 km/hr. Table 1 summarizes the velocity profile data with the baffle in place. Mean velocity was typically within 5% of the 2 km/hr goal and the variation at any traverse point did not exceed 3% of the mean value. Turbulence intensity at this wind speed typically averaged approximately 15%.

Unlike the tests conducted at 2 km/hr, operating the wind tunnel without any baffles at 24 km/hr resulted in a velocity profile which was fairly uniform in the test section. As will be discussed, however, achieving a spatially uniform aerosol concentration in the test section required a slightly different modification of the flow field than was required for the 2 km/hr tests. For the 24 km/hr tests, a 1.22 m (4 ft) square baffle was positioned in the center of the tunnel 8 m upstream of the test section to provide additional aerosol mixing (Figure 4). Fortunately, the presence of this baffle did not adversely affect the velocity profile in the test section. Table 2 summarizes the results of the velocity traverse measurements conducted at 24 km/hr. Mean velocity was typically within 3% of the 24 km/hr goal and the variation at any traverse point did not exceed 5%. Turbulence intensity at this wind speed typically averaged approximately 6%.

### **2.3 AEROSOL GENERATION**

In accordance with 40 CFR Part 40 regulations, both liquid and solid test aerosols must be generated using a vibrating orifice aerosol generator (VOAG). At the EPA-AREAL wind tunnel, monodisperse aerosols were generated using a TSI Model 3050 VOAG equipped with a 20 micron nominal diameter orifice. Liquid flow (0.160 cc/min) through the orifice was provided by a Waters Model 590 HPLC which was independently calibrated at the design flowrate. During operation, the liquid flow rate was continuously monitored using a calibrated variable area flowmeter. The VOAG was routinely operated at a vibrational frequency of 64,000 Hz using a Dynascan Corp. Model 3010 function generator to produce the applied AC signal. The applied vibrational frequency was continuously monitored using a Heath Model SM-2410 frequency counter. By proper selection of liquid feed rate, vibrational frequency, and solution composition, monodisperse aerosols of the required diameter were produced.

For the production of liquid aerosols, the liquid solution consisted of a mixture of oleic acid and uranine dissolved in pure ethanol. Since the liquid flowrate and applied vibrational frequency were typically fixed, the concentration of the nonvolatile oleic acid and uranine in the volatile ethanol solvent was varied to produce particles of the desired

aerodynamic diameter. The mass ratio of uranine to oleic acid in the liquid solution was typically approximately 10%. Following the evaporation of the ethanol, the generated particles consisted of solid uranine powder suspended within liquid oleic acid droplets.

Following their production, liquid droplets were dispersed using a dispersion air flow rate of 1700 cm<sup>3</sup>/min and diluted at a flow rate of 3 m<sup>3</sup>/hr. Because the liquid nebulization process produced droplets which were electrically charged, a Kr-85 based neutralizer (TSI, Model 3054) was used to produce an electrically neutral aerosol. The neutralized aerosols were then introduced into the wind tunnel (Figure 1) through a single 4 inch PVC tube whose outlet is centered vertically in the tunnel. Because the aerosol injection point was immediately downstream of the 57 m<sup>3</sup>/min bypass blower, the aerosol had a tendency to concentrate towards the outside edge of the tunnel. To counteract this effect, a 40.6 cm (16 in) mixing fan was operated adjacent to the aerosol injection zone to direct the aerosol back towards the center of the duct.

The mean aerosol concentration in the test section was measured using a high volume isokinetic sampler (ISO sampler) fitted with a pyramid-shaped nozzle. The sampler was placed in the center of the test section and its inlet nozzle oriented towards the flow. A Gelman Type A/E 20.3 cm x 25.4 cm (8 in x 10 in) glass fiber filter was used in the ISO sampler as the collection substrate. The nozzle was sized to sample 1.13 m<sup>3</sup>/min (40 cfm) isokinetically at the desired wind speed. The duration of the ISO run depended on the expected concentration but typically ranged from 30 min to 60 min. The sample volumetric flow rate was adjusted using a variable transformer that controlled a high-volume sampler motor. Flow was set by monitoring the pressure drop across an orifice at the outlet of the flow system. The orifice itself had been calibrated using a certified top-loading orifice plate (Graseby-Andersen Model# 25, Serial# K-82). The total volume sampled during the ISO was measured using a certified in-line Roots meter (Model# 3M125) fitted with a pressure gauge to correct measured flowrate to actual flowrate at the tunnel operating pressure. Agreement between the flows indicated by the orifice and Roots meter was typically within 1%.

To verify the quality and mean size of the generated aerosols, isokinetic samples were collected in the test section using a specially designed slide impactor. This impactor isokinetically withdrew a representative sample of the aerosol from the test section then impacted the sampled particles on a microscope slide. The slides were pretreated using a solution of 2% NyeBar (Type CT or Type K) oliophobic surfactant which resisted the spread of the oleic acid droplets. Appropriate spread factors for the oil-based oleic acid particles on the oliophobic coating were based on research by Olan-Figueroa et al (1982). Following the aerosol collection, a Nikon Labophot-Pol optical microscope was used to verify that the mean particle size and aerosol uniformity met acceptance criteria outlined in 40 CFR Part 53. The eyepiece micrometer of the microscope was periodically calibrated using a certified stage micrometer (American Optics, Model# 1400).

## 2.4 AEROSOL UNIFORMITY

Regulations governing wind tunnel evaluation of candidate PM<sub>10</sub> samplers requires that the test aerosol within the test section be spatially uniform. Aerosol concentrations must be measured at a minimum of five test points and an acceptable uniformity is defined as a measured coefficient of variation not to exceed 10% at each wind speed. At the EPA-AREAL wind tunnel, particle uniformity was measured with the RAKE which is an array of five isokinetic samplers placed within the test section. Individual RAKE locations are depicted in Figure 5. Each sampler consisted of a commercial 47 mm diameter in-line filter holder with a conical nozzle replacing the usual inlet of the filter holder. Each nozzle projected about 10 cm upstream of the filter holder and was made with a sharp-edged entry leading to a gradually expanding conical section. Separate nozzles were available for conducting uniformity tests at 2, 8, and 24 km/hr. The flowrate through each nozzle was adjusted to provide isokinetic sampling conditions for each windspeed and the air volume sampled by each RAKE sampler was quantified during each test using calibrated dry gas meters. Pressure in the dry gas meters was measured to enable the tunnel operator to correct measured volumetric flowrate to actual volumetric flowrate at the tunnel pressure conditions. Gelman Type A/E glass fiber filters were used in the RAKE samplers due to their acceptable collection characteristics and low background fluorometric content.

While acceptable velocity profiles in the wind tunnel test section at 2 km/hr and 24 km/hr could be achieved using a variety of baffles upstream of the test section, achieving adequate aerosol spatial uniformity in the test section required considerable time and effort. Initially, the generated aerosol was injected approximately 7 m upstream of the test section and a variety of dispersion tubes, mixing baffles, and fan arrangements were used in an attempt to provide the proper uniformity. Since adequate spatial uniformity could not be reliably achieved using this injection point, the entire aerosol generation and dispersion was moved to its present location. The resulting aerosol uniformity was dramatically improved primarily due to the increase in mixing time and intensity. The plywood baffles used to provide proper aerosol uniformity were also effective in providing uniform velocities in the test section.

Tables 3 and 4 summarize the aerosol uniformity tests conducted at 2 km/hr and 24 km/hr, respectively. For 10 micrometer aerosols, the coefficient of variation at the five sampling points was found to be 2.6% and 4.6% at 2 km/hr and 24 km/hr, respectively.

## 2.5 ANALYTICAL TECHNIQUES

Because collected mass deposits were typically too low to accurately quantify gravimetrically, generated aerosols were intentionally tagged with fluorescent material

and quantified fluorometrically. Depending upon the substrate type and its size, various extraction techniques were developed and adopted.

Following aerosol collection, the 47 mm diameter filters from the RAKE nozzles were each placed in labeled, clean, 118 ml polypropylene containers equipped with resealable lids. To each container, 20 ml of 0.01N NaOH was added. The containers were then sealed and placed in a 180 W ultrasonic bath (Branson Cleaning Equipment, Model B-52) for 30 minutes. To ensure that the extract was homogeneous, the contents of each container was then poured into a separate clean 118 ml polypropylene container. Disposable pipettes were then used to transfer an aliquot of each container into separate cuvettes for analysis. The fluorometric content of the solutions was determined using a calibrated Sequoia-Turner fluorometer (Model# 450, Serial# B002610TV). Comparison tests showed that centrifugation of the solutions was not required to ensure reliable test results.

The 20.3 cm x 25.4 cm high volume filters were each carefully folded (using clean forceps) into quarters then placed in clean, 470 ml polypropylene sandwich containers equipped with resealable lids. Either 100 ml or 200 ml (depending upon expected concentration) of 0.01N NaOH was added and each container was ultrasonicated for 30 minutes. The contents of each container was then homogenized by pouring the solution into a clean, separate 118 ml polypropylene container. An aliquot of each solution was then transferred to cuvettes for fluorometric analysis.

To determine sampler aspiration efficiency and particle transport losses within the RAAMP sampler, it was necessary to quantify the aerosol mass deposited on the surfaces of the sampler's various components. Experience has shown, however, that the use of alkaline wash solutions adversely reacts with aluminum surfaces causing the surface to oxidize and corrode with time. The chemical reaction between the aluminum surface has also been found to adversely affect the fluorometric quantitation of collected deposits. Aluminum components, therefore, were extracted by first rinsing (or soaking depending upon component size) with a known volume of distilled water. Occasionally, polyfoam brushes were used to ensure that the collected aerosol was effectively transferred into solution. The collected solution was then buffered to a pH of at least 10 using known volumes of 0.01N NaOH or 0.1N NaOH.

To quantify aerosol deposits within the RAKE nozzles and the ISO nozzles, the outside of the nozzles were first carefully wiped with Kimwipes wetted with absolute ethanol. This step was performed to minimize the chance of sample contamination during subsequent handling of the nozzle. The interior surfaces of the aluminum nozzles were then rinsed with known quantities of distilled water then the wash solution buffered to the proper pH prior to analysis. Because stainless steel nozzles or aluminum nozzles plated with electroless nickel do not adversely react with alkaline wash solutions, these materials were rinsed directly with 0.01N NaOH and the collected wash solutions analyzed fluorometrically.

The aerosol concentration in the wind tunnel is inferred from fluorometric measurements of the uranine concentrations. If the natural content of the glass-fiber filters is significant compared to the collected aerosol mass, then the inferred concentration would significantly overpredict the actual concentration. To quantify the effect of the filter's natural fluorometric content (referred to as a blank), a limited series of tests were conducted. First, three separate 20.3 cm x 25.4 cm (8 in. x 10 in.) filters were extracted per standard procedures. As shown in Table 5, the fluorometric content of these three filters averaged 9 ng of equivalent uranine. For comparison purposes, the ISO sampler was then used to collect 10  $\mu$ m aerodynamic diameter liquid aerosols at two different wind speeds. As indicated in Table 5, the average measured tunnel concentrations for 2 km/hr and 24 km/hr were 55,368 ng and 12,111 ng, respectively. The measured ISO mass concentration at 2 km/hr represents a value approximately 6000 times higher than the 9 ng blank filter value. Similarly, the measured concentration at 24 km/hr represents a mass gain approximately 1300 times higher than the blank filter value. Table 5 also illustrates that the background concentration of aerosols in the wind tunnel (with the aerosol generator turned off) is also insignificant when compared to the typical mass gain experienced during an ISO run. For these reasons, neither blank nor background corrections were made to the measured ISO filter concentrations during the course of the RAAMP project.

Similar tests were performed with the 47 mm Gelman filters used for the RAKE tests. As indicated in Table 6, the mean fluorometric content of ten blank filters was 0.4 ng of equivalent uranine mass. By comparison, the uranine content of aerosols collected during a typical RAKE measurement conducted at 24 km/hr exceeds 400 ng of equivalent uranine mass. Since this value exceeds the blank filter value by a factor of 1000, no corrections for the blank filter were typically made.

### 3.0 STATIC TESTS OF THE RAAMP SAMPLER

#### 3.1 CONDITION CHECK AND FLOW CALIBRATION

Upon receipt of the RAAMP sampler (Sampler #5, RF#21877), a thorough inspection of the sampler was made to check the condition of all critical components. Inspection revealed that no noticeable damage occurred to the unit during shipping and handling and that all operating components appeared to be in good working condition. Prior to use of the sampler, all flow surfaces were cleaned with ethanol-wetted Kimwipes then rinsed with distilled water. A 20 cm x 12 cm impaction substrate was cut from felt material provided by the sampler's manufacturer. As recommended by the manufacturer, this substrate was then saturated using a commercially available motor oil (Castrol Syntec, SAE 5W-50, Part# 072).

The RAAMP sampler was designed to operate at an actual volumetric flowrate of 1.13 m<sup>3</sup>/min (40 acfm) in order to attain the desired cutpoint within the sampler. Flow control within the sampler was provided by a volumetric flow controller (Graseby-Andersen Model# 76-100, Serial# P1833) which operates under choked flow conditions. The actual flow rate achieved by the device can be estimated using look-up tables (provided by Graseby-Andersen) based on ambient pressure, ambient temperature, and pressure drop across the sampler's afterfilter. As part of these preliminary tests, the unit's flow controller was calibrated in the laboratory using a certified high volume calibration orifice (Graseby-Andersen Model # 25, Serial# K-82).

Table 7 presents the results of this calibration using a Gelman Type A/E glass fiber afterfilter in the RAAMP sampler. Calibration performed on two separate days indicated that the RAAMP sampler's actual flow of 1.178 m<sup>3</sup>/min was approximately 4% higher than the desired 1.13 m<sup>3</sup>/min flowrate. However, the predicted flow (using the look-up tables) agreed closely with the calibrated flow. For these near-standard temperature and pressure conditions, the predicted flow underestimated the calibrated flow by approximately 1%.

#### 3.2 PARTICLE SIZE CALIBRATION TESTS

At the time the RAAMP sampler was received, facility work in and around the wind tunnel precluded wind tunnel evaluation of the sampler. To provide a preliminary measure of the sampler's performance, a limited series of particle size calibration tests was performed. Unlike the wind tunnel tests, these performance tests were conducted under near-static (still air) conditions and thus did not simulate the sampler's performance during field use.

For these tests, a chamber 1.22 m wide x 1.22 m deep x 2.44 m high was built to enclose the entire RAAMP sampler. Monodisperse calibration aerosols were generated

outside the chamber and introduced near the top of the chamber approximately 45 cm from the RAAMP sampler inlet. At the RAAMP mean flowrate of 1.178 m<sup>3</sup>/min, mean downward velocity of the challenge aerosol through the chamber was calculated to be approximately 1.3 cm/sec. Excess aerosol was exhausted from the chamber through a flexible pipe.

Regulations regarding wind tunnel performance tests define sampler effectiveness as the ratio of concentration measured by the sampler's afterfilter (mass divided by sampled volume) to that concentration measured in the wind tunnel. Since the concentration of the small test chamber could not be accurately quantified, the concentration of the challenge aerosol could only be estimated by quantifying aerosol deposits on the internal surfaces of the RAAMP sampler. For these tests, three sections of the RAAMP sampler were separately analyzed for mass deposits. Specifically, these sections were the top of the impactor stage (including the walls of the rectangular nozzles), the impaction filter, and the afterfilter. Because test aerosols consisted exclusively of liquid oleic acid aerosols tagged with uranine, the oiled impaction filter was considered unnecessary and was replaced with an equivalent sized Gelman Type A/E glass fiber filter.

For these tests, test aerosols of 5, 7, 9, 10, 11, 13, and 20 micrometer aerodynamic diameter (nominal) were generated using the VOAG. For each size generated, aerosol samples were collected on NyeBar-coated microscope slides and the quality of the aerosols verified using an optical microscope. The size distribution of the generated aerosol was not measured, however, so no effectiveness corrections could later be made for the presence of multipllets in the calibration aerosol. Following a 60 minute run time, the impaction filter and afterfilter were removed and placed in separate containers of 200 ml distilled water. These containers were then sonicated for 5 minutes prior to analysis. Kimwipes wetted with distilled water were used to wipe the top surface of the impactor and the walls of the rectangular nozzles. The Kimwipes were then immersed in 40 ml of distilled water and sonicated for 50 minutes prior to analysis. All extracted solutions were then centrifuged for 5 minutes and analyzed using a calibrated SLM Aminco Fluoro-Colorimeter II.

For these tests, sampler effectiveness was operationally defined as the ratio of the mass collected by the afterfilter to the total mass collected by the afterfilter plus the impactor plate plus the material collected during the plate wipe. In essence, this approach estimated the fractionation characteristics of the impaction jets themselves rather than that of the complete sampler. Note also that this approach assumed that aerosol losses were negligible on the underside of the impaction jets and in the region between the impaction plate and the afterfilter.

Figure 6 summarizes the results of the effectiveness tests conducted under these static conditions. From the data, it can be seen that the effectiveness of the impaction stage was a monotonic function of particle size and that the effectiveness was

approximately 50% at 10.5 micrometers aerodynamic diameter. It should be reiterated, however, that this data represented the performance of the impaction stage itself and cannot be reliably extrapolated to predict the sampler's overall performance at wind tunnel or field conditions.

## 4.0 WIND TUNNEL TESTS OF THE RAAMP SAMPLER

### 4.1 EXPERIMENTAL SETUP

At the time the RAAMP sampler was received for testing, dimensions of the wind tunnel test section access doors would only allow testing of candidate samplers no wider than approximately 51 cm (20 in). Since the dimensions of the RAAMP instrument case measured approximately 61 cm x 65 cm, modifications to the test section were required before evaluation of the RAAMP sampler could begin. To accommodate the RAAMP sampler, therefore, the access door, viewing windows, test section frame, and wind tunnel floor were all modified to allow testing of samplers up to 81 cm wide.

The RAAMP sampler consisted of an omnidirectional inlet mounted on top of an instrument case which housed the vacuum pump and control components. Since the inlet was not centered over the top of the housing, however, orientation of the sampler relative to the mean wind direction may have an effect on the overall performance of the sampler. Consideration was given at this time, therefore, as to which orientation in the wind tunnel would best simulate its intended field use. Discussions with the sampler's manufacturer revealed that the sampler will be mounted on telephone poles during field tests in such an orientation that the prevailing wind direction would be directed normal to the side of the instrument case. As shown in Figure 7, this orientation was adopted for performance testing of the sampler in the wind tunnel. Plywood shims were used to fill in the gaps in the tunnel floor around the RAAMP sampler. Note also from Figure 7 that the sampler was positioned such that the inlet was centered horizontally in the test section. This horizontal location was identical to that of the 1.13 m<sup>3</sup>/min ISO sampler used to determine mean wind tunnel aerosol concentrations. The location of the RAAMP sampler was such that the leading edge of the sampling inlet was coincident with the vertical plane (normal to the mean flow direction) sampled by the ISO sampler and the RAKE samplers.

Consideration was also given to the vertical placement of the RAAMP sampler in the wind tunnel. Since the overall 180 cm height of the sampler exceeded the 122 cm height of the test section, it was obvious that only a portion of the sampler could be tested in the wind tunnel. Since the relative size and close proximity of the instrument housing relative to the inlet was believed to have some effect on overall sampler performance (especially aspiration efficiency), it was considered necessary to operate the sampler with as much of the housing exposed in the wind tunnel as allowed by regulations. Federal regulations governing wind tunnel testing of size-selective inlets specify that blockage by the sampler (or portion thereof) must not exceed 15% of the test section's cross-sectional area normal to the mean wind direction. Based on this consideration, therefore, the sampler was mounted on a 21 cm high cart equipped with wheels for easy movement of the sampler in and out of the test section. Blockage of

the sampler (including the sampling inlet and flow tube) in this arrangement was exactly 15%. As shown in Figure 8, this vertical positioning of the sampler placed the lower leading edge of the inlet at the vertical center of the test section matching the vertical position of the ISO sampler. Because the vertical, horizontal, and longitudinal positions of the ISO and RAAMP sampling inlets was identical, the two systems should experience similar freestream flow conditions and aerosol concentrations. In addition, the fact that the ISO and RAAMP systems sample at nearly identical flowrates also made interpretation of resulting wind tunnel performance data much more straightforward.

## 4.2 EXPERIMENTAL PROCEDURES

The primary purpose of Phase 1 of the project was to perform a preliminary evaluation of the RAAMP sampler to ascertain whether its overall size-selective characteristics made it a viable candidate for submission for full-scale PM10 performance tests. Since full-scale 40 CFR Part 53 tests were not to be performed at this time, the regulation's strict test protocol and procedures were amended to optimize the information gathered in the laboratory. For instance, performance testing regulations required that the spatial uniformity of test aerosols in the test section be measured daily before each test series. During this preliminary evaluation, however, these spatial uniformity tests were only performed periodically to verify the operating condition of the wind tunnel. Since the operating conditions of the wind tunnel (tunnel geometry, baffle arrangement, flow rate, aerosol dispersion, etc.) did not vary from day to day, significant variations in spatial uniformity were not been observed with time.

To date, performance tests of the RAAMP sampler have been conducted using test aerosols composed exclusively of liquid 10 micrometers aerodynamic diameter. Because regulations required that EPA approved PM10 samplers display 50% effectiveness at  $10 \pm 0.5$  micrometers, 10 micrometers was the particle size of the greatest interest. In addition, this particle size normally corresponds to the sharp part of a candidate sampler's effectiveness curve thus providing a good measure of the overall position of the curve with respect to the sampler's 50% effectiveness value. Finally, the use of liquid aerosols was justified for these tests as liquid aerosols characteristically display greater sticking efficiency than do solid aerosols and thus display higher transport losses within a sampler.

Furthermore, tests to date have been confined to characterization of the RAAMP sampler at wind speeds of 2 km/hr and 24 km/hr. Experience has shown that size-selective sampler performance is normally a monotonic function of windspeed with sampler effectiveness an inverse function of wind speed. The 2 km/hr and 24 km/hr test results, therefore, typically encompass the 8 km/hr performance data. Wind tunnel tests at 8 km/hr will later be performed on an as-needed basis.

A typical test protocol for the RAAMP sampler evaluation was as follows. At the

start of the day, ambient temperature and pressure conditions were measured and recorded. Checks were then made to ensure that the wind tunnel was ready to operate and that all mixing fans and flow dampeners were operating and in the correct orientation. The wind tunnel bypass chilled water supply was turned on and the chiller blower activated. The tunnel's primary blower was turned on and its rotational speed adjusted to attain the desired windspeed. Following a 15 minute warm-up period, the wind tunnel air temperature and relative humidity were measured and recorded.

The monodisperse aerosol generator was then brought on-line and allowed at least 30 minutes to stabilize. Aerosol was then introduced into the tunnel and a representative sample collected on the slide impactor during a sampling time of at least 5 minutes. The aerosol quality was then verified using the optical microscope and any necessary adjustments were made to the aerosol generation and dispersion system. The aerosol concentration in the wind tunnel was then allowed to stabilize for at least 15 minutes before sampling began. Throughout the day's operation, aerosol samples were periodically extracted and the aerosol quality verified.

Sampling would normally begin using the 1.13 m<sup>3</sup>/min ISO sampler to determine mean tunnel concentration. Prior to sampling, a new high-volume filter was installed in the sampler and a clean sampling nozzle installed. The Roots meter initial reading was recorded and checked against the previous day's final reading. Based on the measured tunnel air temperature and ambient pressure, a calculation was made of the flow orifice pressure required for the ISO sampler to achieve a volumetric flowrate of 1.13 m<sup>3</sup>/min. The ISO sampler was then installed within the wind tunnel and representative sampling begun. Run times for the ISO sampler depended upon expected aerosol concentration but typically ranged from 30 to 60 minutes. At the end of the sampling period, the sampler was turned off, removed from the wind tunnel, and the Roots meter final volume recorded. The inlet nozzle and high-volume filter were then removed and their collected aerosol deposits extracted and quantified fluorometrically using procedures previously described. Mass concentration (as uranine in µg/m<sup>3</sup>) of the aerosol collected by the ISO sampler was then calculated as the collected aerosol uranine mass divided by the pressure corrected Roots meter displaced volume.

During the ISO run, the RAAMP sampler was prepared for subsequent operation within the wind tunnel. A clean glass fiber filter was loaded in the afterfilter assembly and the assembly installed within the instrument housing. When the ISO run was completed, the RAAMP sampler was then installed in the test section, turned on, and operated for a duration not less than that of the previous ISO test. At the completion of the test, the RAAMP sampler was turned off, removed from the wind tunnel, and its afterfilter removed and analyzed for collected aerosol mass. Mass concentration (as uranine in µg/m<sup>3</sup>) of the aerosol collected by the afterfilter was then calculated as the collected mass divided by the calibrated flowrate divided by the sampling time. Fractional effectiveness of the RAAMP sampler was then calculated as the ratio of the

RAAMP measured afterfilter concentration divided by the ISO measured concentration.

### **4.3 EFFECTIVENESS CHARACTERISTICS OF THE RAAMP SAMPLER**

Preliminary operation of the RAAMP sampler at tunnel wind speeds of both 2 km/hr and 24 km/hr provided early indications that the current version of the sampler would not meet 40 CFR Part 53 acceptance criteria for PM10 size selective inlets. For the 10 micrometer aerodynamic test aerosols, average effectiveness of the sampler at a tunnel windspeed of 2 km/hr was measured to be approximately 30%. At a windspeed of 24 km/hr, effectiveness of the sampler challenged with the same aerosol dropped to approximately 13%. Because these test results suggested that design modifications to the sampler would be necessary, continued testing of the sampler using particles of different aerodynamic diameters was not performed. After consultation with the sampler's manufacturer, efforts were focussed on investigating the reasons that the sampler exhibited lower effectiveness than desired.

The overall effectiveness of an ambient PM10 aerosol sampler is an interrelated function of three distinct phases of a sampler's operation. To accurately characterize an airborne aerosol sample in a flowing airstream, the sampler must first extract a representative aerosol sample from that airstream both in terms of particle size and concentration. Aspiration efficiency is the generally accepted term for the ratio of the mass concentration crossing the sampler inlet to the mass concentration existing in the freestream atmosphere. For ambient samplers, extensive theoretical and experimental studies have shown that aspiration efficiency is generally a function of particle size, wind speed, wind direction, turbulence intensity, sampling flowrate, and inlet geometry and dimensions.

Accurate size characterization of ambient aerosols also requires that aspirated particles be efficiently transported from the sampler's inlet to its size fractionating section. Significant losses of particles to internal surfaces of the sampler can result in dramatically reduced overall effectiveness. Transport losses of supermicron particles is generally a function of internal geometry, sampling flowrate, turbulence intensity, particle size, and particle composition.

The final phase of the sampler's operation involves its size-selective section which separates the incoming aerosol into two distinct size fractions based on the particle's inertial properties in the flowing airstream. Overall performance of the sampler can be significantly degraded due to problems associated with the size-fractionating component. These problems may be associated with the sampler's overall design or may be associated with operational problems such as particle bounce, particle deagglomeration, or stage overloading.

An ideal PM10 size-selective sampler's design and operation would optimize all three of the phases of operation. This hypothetical sampler would display 100%

aspiration efficiency independent of the aerosol characteristics and independent of the ambient conditions. In this ideal sampler, all aspirated particles would then be transported efficiently to the size-selective stage where they would be fractionated efficiently into the desired size components. In actuality, however, samplers which meet 40 CFR Part 53 acceptance criteria may display only fractional aspiration efficiency, fractional transport efficiency, and efficient size fractionation. It is the proper combination of these sampling parameters which results in overall sampler performance of the desired characteristics.

#### 4.4 ASPIRATION CHARACTERISTICS OF THE RAAMP SAMPLER

Since the RAAMP sampler displayed overall effectiveness values of 30% and 13% at wind speeds of 2 km/hr and 24 km/hr, respectively, some design modifications would be needed in order to improve the sampler's performance. In order to properly address design changes, however, it is first necessary to know which of the three phases (aspiration, transport, or fractionation) required attention. In order to properly diagnose the RAAMP sampler's performance, therefore, a series of mass balance tests was conceived and conducted in the laboratory. For these tests, the sampler's inlet section, transport section, and fractionation section were carefully disassembled and thoroughly cleaned using ethanol then were rinsed with distilled water. Wetted surfaces of these components (i.e. surfaces which can potentially come in contact with sampled aerosol) were identified and subjected to additional cleaning. As depicted in Figure 9, these surfaces included the interior of the inlet head (including the deflection cone), inlet screen, 7.6 cm diameter tube, expansion section, impaction stage (including the impactor jets), impaction plate, impactor plate filter, top of the filter assembly, and the afterfilter. These individual components were then separately analyzed for their background fluorescent content. Some surfaces required additional cleaning until an acceptable background level was achieved. The components were then dried, reassembled, and the sampler prepared for testing. In order to eliminate the possible analytical interference of the Syntec motor oil for these mass balance tests, the oil impregnated impaction plate filter was replaced with an ungreased Gelman Type A/E glass fiber filter of the same dimensions. Since the liquid test aerosols display virtually 100% sticking efficiency on this ungreased surface, this approach was justified and should accurately simulate the behavior of the normally oiled impaction surface.

Mass balance tests were first conducted at a wind speed of 2 km/hr using the 10 micrometers aerodynamic diameter aerosol. Per standard procedures, the ISO sampler was first operated in the wind tunnel for 30 minutes to measure the mean aerosol concentration. Mean aerosol concentration measured during this test was  $1.72 \mu\text{g}/\text{m}^3$  as measured by the ISO sampler. The RAAMP sampler was then operated for an extended period of 180 minutes in order to collect quantifiable aerosol deposits on all surfaces of

interest. At the end of the time period, the sampler was removed from the tunnel and the components carefully removed from the sampler. Aerosol deposits were extracted from all surfaces and individually quantified using the same techniques employed during the background tests.

Test results for the 2 km/hr tests are summarized in Table 8. Listed are the equivalent aerosol concentrations (measured mass per sampled volume) for each of the eight components of interest. Of particular interest is the sum of the concentration for all components versus the measured mean concentration. In effect, this represents the aspiration efficiency of the sampler for the 10 micrometer aerosols at this wind speed. As shown in the table, overall measured concentration was  $1.98 \mu\text{g}/\text{m}^3$  indicating a 115% aspiration efficiency when compared to the tunnel's  $1.72 \mu\text{g}/\text{m}^3$  concentration. Also calculated was the sampler's effectiveness value of 29% which agreed with previous performance tests of the sampler at this wind speed.

In addition, the percentage of the total mass sampled was calculated for each measured component which was of value in determining transport efficiency and impactor stage efficiency. Of the total aerosol sampled at this wind speed, 14% of the mass was lost to the inlet screen. Losses to the head, transport tube, and expansion section were somewhat negligible and totalled approximately 5%. Losses to the impaction stage (including upper surfaces, jet throats, and lower surfaces), however, represented 25% of the total sampled mass. Losses in the region downstream of the impaction plate and upstream of the afterfilter were measured to be 8%.

These mass balance tests of the RAAMP sampler were then conducted at a wind speed of 24 km/hr using the same particle size and the same operating protocols used for the 2 km/hr tests. For this test the high volume ISO sampler was operated for 30 minutes and measured a tunnel concentration of  $0.196 \mu\text{g}/\text{m}^3$ . As shown in Table 9, summation of component mass concentrations led to an overall concentration of  $0.230 \mu\text{g}/\text{m}^3$ . This 117% aspiration efficiency is similar to the 115% measured at the 2 km/hr wind speed. The calculated sampler effectiveness value of 14% agrees closely with previous measurements at this wind speed.

Inspection of the fractional aerosol losses to each of the wetted components was again quite instructive from a diagnostic perspective. Of the total aerosol sampled by the sampler at this wind speed, 45% of the mass was lost to the inlet screen. To explain this dramatic increase in transport losses compared to those experienced at 2 km/hr, it was speculated that the incoming air at 24 km/hr entered at a more tangential angle than occurred during the 2 km/hr tests. This hypothesis was supported by the observation that particle losses to the inlet's head increased from 0% at 2 km/hr to 19% at 24 km/hr.

Similar to the 2 km/hr tests, losses in the inlet tube and expansion section represented only 4% of the aspirated aerosol mass. Because penetration through the screen and inlet were much lower at 24 km/hr, losses in the impactor jets represented only 9% of the total aerosol sampled. As will be discussed, however, fractional losses in

the impaction stage and other downstream components were relatively independent of windspeed.

Particle losses to the inlet screen in the RAAMP obviously were unacceptably high and need to be addressed during upcoming modifications to the sampler. Based on inertial impaction of incoming particles on the screen's wires, the screen losses can theoretically be predicted. The existing screen of the RAAMP sampler has a mean wire diameter of approximately 0.07 cm diameter. Assuming an approach velocity equal to the 54 cm/sec suction velocity of the inlet (ignoring wind speed effects), the resulting Stokes number is approximately 0.50. Modeling the screen wires as cylinders aligned normal to the flow and incorporating collection efficiency curves of Golovin and Putnam (1962), the screen's measured 45% closed area would lead one to predict up to 16% inertial losses of 10 micrometer aerodynamic diameter particles. This predicted loss value is close to the 14% value measured during the 2 km/hr performance tests. Incidentally, the mean suction velocity of the RAAMP sampler (flowrate divided by inlet area) was approximately equal to the tunnel velocity of 2 km/hr. Adopting an approach velocity of 24 km/hr, one would predict screen losses up to 41%. The agreement between this prediction and the measured 45% losses at 24 km/hr might support the hypothesis that the incoming airstream enters tangentially at 24 km/hr and would thus best represent the approach velocity for these loss predictions.

The observation that the overall aspiration efficiency of the RAAMP sampler was approximately 115% at both 2 km/hr and 24 km/hr is of interest from a diagnostic perspective. Extensive theoretical and experimental investigations of inlet aspiration efficiency have been conducted with relatively simple inlet geometries such as thin-walled nozzles of circular cross-section. These investigations have shown that aspiration efficiency is function of inlet Stokes number, turbulence intensity, inlet orientation relative to the local flowfield, and ratio of the inlet suction velocity to the freestream velocity at the point of sampling. While accurate predictive models have been developed for these classic sampling nozzles, the RAAMP inlet's complex geometry and low suction to freestream velocity ratio makes direct application of these models of limited value from a quantitative sense. From a qualitative perspective, however, these investigations can be used as a basis for understanding the RAAMP inlet's aspiration characteristics.

Modeling the RAAMP inlet as a single sharp-edged nozzle sampling anisoaxially 90° to the approaching freestream, it is possible to predict aspiration efficiencies up to 100% if the inlet's Stokes number is sufficiently low. Hangal and Willeke (1990) developed equations to predict aspiration efficiency at 90° anisoaxial sampling conditions for freestream velocities up to twice that of the suction velocity. Using these equations to predict the RAAMP inlet's aspiration characteristics for 10 micrometer aerodynamic diameter aerosols at this maximum velocity ratio, one would predict aspiration efficiencies from 93% to 97% depending upon one's choice of the inlet characteristic

dimension during calculation of the Stokes number. Under no combination of Stokes numbers and velocity ratio, however, is it possible to predict aspiration efficiencies greater than 100% at this 90° anisoaxial orientation.

Since the observed enrichment in freestream concentration can only occur at anisoaxial orientations less than 90°, it was hypothesized that the configuration and close proximity of the RAAMP instrument case may have adversely affected the flowfield in the region of the inlet. Limited flow visualization (using a tuft wand) confirmed that the bluff instrument case was forcing a portion of the incident airstream up towards the sampling inlet resulting in incident angles less than 90°. This observed behavior possibly accounted for the increased aspiration efficiency. To further test this hypothesis, modifications were made to the experimental setup in the wind tunnel to isolate the sampling inlet from the influence of the instrument case. This modification was achieved by installing a horizontal plywood baffle at the top of the instrument case. This baffle extended approximately 140 cm upstream and 45 cm downstream of the instrument case. Flow visualization at wind speeds of both 2 km/hr and 24 km/hr confirmed that this modification was very effective in removing the adverse effect of the instrument case on the flow field in the immediate vicinity of the inlet.

Following this modification, the mass balance tests of the RAAMP sampler were repeated at a wind speed of 2 km/hr. As shown in Table 8, removing the influence of the instrument case reduced the aspiration efficiency from 115% to 97% which was a value close to the predicted 93% to 97% value for this sampling orientation. Note also that the fractional particle losses to the RAAMP inlet screen were appreciably reduced from 14% to 10%. Prior to the modification, the adverse flow trajectory caused by the instrument case may have resulted in higher turbulent deposition losses in this region. Lastly, despite the lower aspirated aerosol concentration observed in this configuration, the lower screen losses counteracted this reduction resulting in no significant change in overall sampler effectiveness.

These tests using the modified flow configuration were also repeated at a wind speed of 24 km/hr. As shown in Table 9, the modified setup reduced the aspiration efficiency from 117% to 100%. Unlike the 2 km/hr tests, however, no significant decrease in screen losses was observed at the 24 km/hr windspeed with screen losses accounting for 43% of the aspirated aerosol mass.

Because screen losses were prohibitively high in both configurations, these mass balance tests were also conducted with the inlet screen removed from the sampler. Tests conducted at a wind speed of 2 km/hr (Table 8) confirmed that overall sampler effectiveness increased as expected due to the increased penetration of aspirated aerosols into the sampler's transport and fractionation sections. As shown in Table 9, removal of the inlet screen resulted in an increased sampler effectiveness from 13% to 23% at a wind speed of 24 km/hr. Particle losses to the sampling head were 26% of the aspirated aerosol mass indicating that the head's design needs to be addressed during future

redesign of the RAAMP sampler.

#### 4.5 PARTICLE TRANSPORT CHARACTERISTICS OF THE RAAMP SAMPLER

As has been discussed, excessive transport losses within an ambient size-selective sampler can significantly reduce the sampler's overall performance. In the RAAMP sampler, transport losses can occur to any of the following components: inlet head, screen, transport tube, transition section, impactor stage, impactor plate, or filter top assembly. The particle loss of the sampler's inlet head and inlet screen were discussed in detail in the previous section. Losses to the sampler's remaining downstream components will be discussed in this section.

Aspirated aerosol which penetrates the RAAMP sampler inlet screen and inlet head is then transported into the 48 cm long, 7.6 cm diameter cylindrical tube which conveys the aerosol downward towards the sampler's fractionation section. Although particle losses can occur by a number of distinct mechanisms (gravitational settling, electrostatic deposition, etc.) turbulent inertial deposition is probably the dominant loss mechanism in the RAAMP transport tube. Turbulent deposition occurs when stream turbulence propels an airborne particle through the laminar sublayer of the transport tube where it can be collected on the tube's walls. Liu and Agarwal (1974) developed empirical predictive models to predict turbulent losses in tube flow as a function of Stokes number, Reynolds number, tube diameter, and tube length. Using these models to predict 10 micrometer aerodynamic diameter particle losses in the RAAMP sampler under typical operating conditions (Reynolds number of approximately 22,000) leads to the prediction that less than 1% of these aerosols would be lost in this section.

As summarized in Table 10, actual losses in the transport tube at wind speeds of 2 km/hr were measured to be approximately 3% and were relatively independent of the proximity of the inlet screen or instrument case. Measured losses are defined as the aerosol mass deposited on the component divided by the total mass encountered by the component. The slightly higher than predicted losses in the tube were probably due to entry effects near the inlet head region where acceleration into the smaller diameter tube must occur. The empirical loss models of Liu and Agarwal do not account for tube entry losses and thus would underpredict overall tube losses. This entry loss hypothesis is supported by the observation that tube transport losses increased to approximately 8% at a wind speed of 24 km/hr. Overall transport losses within the tube increased to 15% when the inlet screen was removed from the sampling inlet due to the increased fraction reaching the tube.

Aerosol successfully transported through the inlet tube may next be lost to interior surfaces of the transition section between the inlet tube and the impactor stage. As shown in Table 10, particle losses to this section were measured to be approximately 2%

and were relatively independent of windspeed and sampler configuration. Losses to the expansion section, therefore, may be considered to have a negligible effect on the RAAMP sampler's overall effectiveness.

Particle losses can next occur in the sampler's impaction section with losses occurring on the stage's top surface, impactor jet walls, and/or on the stage's bottom surface. Unlike losses to the sampler's transition section, however, losses to the impactor section were found to be significant. As shown in Table 10, particle losses averaged 26% of the challenge aerosol mass and were relatively independent of wind speed and sampler configuration. This lack of dependence can be expected since flow field dynamics upstream of the sampler's transition section have little effect on downstream losses.

To further characterize losses to the impactor stage, a single test was conducted with the plate's upper surface, jet walls, and lower surface independently analyzed for collected mass deposits. Test results suggested that approximately half the aerosol losses to this component occurred on the top surface with the remaining 50% equally distributed between the jet walls and the underside. Since it was speculated that the losses to the upper surface may be due to the upstream transport tube acting as a single stage impactor with this surface acting as the collection plate, a calculation was made of the jet's theoretical cutpoint. Using predictive equations developed by Marple and Willeke (1976), the calculated 25 micrometer aerodynamic diameter cutpoint suggested that direct impaction may only account for a fraction of the observed 10 micrometer losses in the region. Losses in this region were probably due primarily to the necessary convergence of the airstream from the transition section into the sharp-edged rectangular nozzles. In addition to these nozzle entry losses, transport losses to the nozzle walls may also be attributed to the sharp-edged geometry of the rectangular nozzles.

Lastly, particle transport losses can occur in the RAAMP sampler in the region between the impaction plate and the afterfilter. Similar to the transition losses, these measured losses were somewhat variable but averaged approximately 18% of the total mass exiting the impactor plate region. While these losses were not prohibitively high, this region may need to be addressed during redesign of the overall sampler.

#### **4.6 FRACTIONATION CHARACTERISTICS OF THE RAAMP SAMPLER**

In addition to providing information regarding aspiration characteristics and transport efficiency, the mass balance tests performed under the various test conditions also allowed characterization of the size fractionation section of the RAAMP sampler. Table 11 presents a summary of the calculated impactor efficiency results where stage efficiency is defined as the mass collected on the impactor plate divided by the total mass collected on the impactor plate, filter assembly, and afterfilter. Because particle losses to the underside of the impactor stage were normally not quantified separately, this

calculation does not include these losses. As can be seen in the table, the measured efficiency averaged approximately 40% and was relatively independent of wind speed or inlet flow configuration.

Table 11 also summarizes the measured penetration characteristics of the size fractionation section of the RAAMP sampler. For these calculations, filter penetration was defined as the collected afterfilter mass to the total mass measured downstream of the impactor jet exit plane. As before, losses to the underside of the impactor stage were not considered in this calculation. Calculation results showed that the penetration of the fractionation section was close to 50% and was again relatively independent of windspeed or inlet flow configuration. This result suggests that redesign of the fractionation section may not require immediate attention and that more emphasis should be placed on improving the sampler's aspiration characteristics and aerosol transport efficiency.

## **5.0 WIND TUNNEL TESTS OF THE MODIFIED IMPACTOR STAGE AND TRANSITION SECTION COMPONENTS**

### **5.1 INTRODUCTION**

Wind tunnel evaluation of the original RAAMP sampler design revealed that particle losses to the impactor stage were unacceptably high. As discussed, fractional losses to the impactor stage were approximately 28% and were relatively independent of wind speed. In an effort to reduce these losses, the transition section (between the transport tube and the impactor stage) and the impactor stage were both redesigned by the manufacturer. This report summarizes the wind tunnel evaluation of these modified components.

In the RAAMP sampler, the function of the transition section is to decrease the velocity of the airstream which exits the 7.6 cm diameter transport tube. In the original design, this component had outlet dimensions of 21cm long by 17.6 cm wide. Outlet dimensions of the new transition section have been reduced and were measured to be approximately 17.6 cm long by 11.4 cm wide.

In the original impactor stage design, the rectangular nozzles had a sharp-edged entry and a fully developed throat length of approximately 0.66 cm. In the new impactor stage design, the entrance of the jets has been tapered at an angle of approximately 60° with a fully developed throat length of approximately 0.16 cm. Other critical stage parameters (i.e. jet widths, jet spacing, and number of jets) were not modified in the new design.

To allow direct comparison with previous wind tunnel tests, these tests were conducted using 10 micrometer aerodynamic diameter aerosols in conjunction with a tunnel wind speed of 2 km/hr. The flow separation baffle was also in place during these tests to eliminate the effect of the instrument case on inlet performance. The RAAMP sampler was operated with the inlet screen removed from the head assembly.

### **5.2 EVALUATION OF THE MODIFIED IMPACTOR STAGE**

To individually evaluate the effect of each new component on overall impaction stage losses, wind tunnel tests were first conducted with the new impactor stage in conjunction with the original transition section. Table 12 presents mass balance test results of the sampler in this configuration. For this single test, aspiration efficiency of the sampler was measured to be 103% and overall sampler effectiveness measured 59%. This sampler effectiveness represents a fairly dramatic increase compared to the original sampler's effectiveness of 34% at the same wind speed.

To account for this observed increase in effectiveness, individual losses to the various components of the RAAMP sampler are summarized in Table 13. As expected

(based on previous Phase 1 results) particle losses to the transport tube and transition section were found to be negligible. Losses in the new impactor stage were measured to be 17% of the challenge aerosol which is a significant reduction from the 28% measured in the original impactor stage (see Table 10). These reduced losses, however, only partially account for the increased sampler effectiveness measured during this test.

Table 13 illustrates that the particle collection characteristics of the impactor stage have been appreciably altered by tapering the entrance of the impactor jets. Impactor stage efficiency of the new design is approximately 18% compared to the 41% measured with original impactor stage (see Table 11). This reduction in stage efficiency is thought to be due to a combination of two factors. First, there exists a significant reduction in the ratio of the jet's throat length to jet width (T/W) from approximately 1.2 in the original stage design to approximately 0.28 in the modified design. In the modified design, the incoming particles may have insufficient time to accelerate to the fluid velocity at the jet exit. This phenomenon would result in reduced particle stopping distance and thus reduce the impaction efficiency of the stage.

A second possible explanation for the observed reduction in stage efficiency regards differences in the fluid flow field in the region of the jet entrance. In the original stage design, the sharp-edged geometry of the jet entrance may have resulted in the formation of a fairly prominent vena-contracta in the jet throat. The presence of the vena-contracta would have resulted in a higher jet exit velocity than would be predicted simply by dividing the sampler's volumetric flowrate by the jet area. In the modified stage design, however, the significant taper of the jet entrance may have established a wider vena-contracta resulting in lower jet exit velocity. Reduced particle stopping distance and thus reduced stage efficiency would have been a direct result of this lower exit velocity.

While losses to the impactor stage have been measurably reduced, further reductions will probably be necessary during further redesign of the sampler. Since losses to the underside of the impaction plate may represent a significant fraction of the total stage losses, this region of the sampler may require further attention. Losses to the sampler's top assembly (approximately 16%) were unaffected by the new stage design will also require attention during redesign of the sampler.

### **5.3 EVALUATION OF THE MODIFIED TRANSITION SECTION**

These mass balance tests were then conducted using the new impactor stage in conjunction with the new transition section. As depicted in Table 12, sampler aspiration efficiency was measured to be 92% for this single test. Overall sampler effectiveness for this test setup was measured to be 44%.

Table 13 accounts for the observed reduction in sampler effectiveness from 59% (with the original transition) to 44% (with the new transition). Note that transport tube

losses, transition losses, impactor stage losses, and filter top assembly losses are approximately equal for the tests performed with the two transition sections. Impactor stage efficiency, however, increased from approximately 18% with the original transition section to approximately 24% with the new transition section. This reduction in stage efficiency accounts for the observed reduction in overall sampler effectiveness. While the exact reason for the observed difference in stage performance is unclear, the difference probably occurs due to a change in the flow distribution through the 13 impactor jets. Changes in flow distribution would result in changes in individual jet performance and thus could account for the observed overall increase in efficiency.

## 6.0 WIND TUNNEL TESTS OF THE MODIFIED INLET

### 6.1 INTRODUCTION

As discussed, wind tunnel testing of the RAAMP sampler included a performance evaluation of the sampler's inlet. Tests conducted at wind speeds of 2 km/hr and 24 km/hr suggested that the inlet's aspiration characteristics were acceptable but that losses to the inlet's screen and internal surfaces were unacceptably high. In an effort to reduce these losses, the inlet of the RAAMP sampler was redesigned by the manufacturer. To accommodate the new inlet's geometry and to further reduce particle losses, the transport tube of the RAAMP sampler was also redesigned. This report summarizes the wind tunnel evaluation of these modified components.

The redesigned inlet consists of a rectangular cover (27 cm x 21 cm) suspended approximately 5 cm over the entrance of the transport tube. Flow deflectors (Figure 10) were included to direct a portion of the incoming aerosol downward towards the vertical axis of the transport tube. The transport tube has a rectangular cross-section with dimensions of approximately 17 cm by 11.5 cm. The major axis of the transport tube's cross-section corresponds to that of the rectangular cover. To minimize the effect of the RAAMP sampler case on the inlet performance, the transport tube was designed with a length of approximately 79 cm. This compares to a transport tube length of 48 cm in the original RAAMP sampler design.

Prior to evaluating the new inlet in the wind tunnel, some modifications of the experimental setup were required. If attached directly to the top of the RAAMP case, the new inlet would have extended to an elevation in the test section considerably higher than that used for previous evaluation of the RAAMP sampler. Since neither the fluid flow field nor the aerosol concentration had previously been characterized at this extreme elevation, considerable uncertainty would have resulted regarding subsequent test results. To minimize this uncertainty, the length of the new transport tube was shortened to approximately 43 cm. This modification placed the inlet in the vertical center of the test section which is identical to the point sampled by the ISO sampler and previous RAAMP sampler designs. To prevent the anticipated adverse effect of the instrument case on inlet's performance, subsequent tests were performed with the horizontal flow separator installed (Figure 2).

Tests of the new inlet were conducted in conjunction with the newer impaction stage containing the taper jet inlets. To allow direct comparison with previous wind tunnel test results, these tests were conducted using 10 micrometer aerodynamic diameter liquid aerosols. Mass balance tests of the new RAAMP sampler configuration were

conducted at wind speeds of 2 and 24 km/hr. Following extended run times, aerosol mass deposits were quantified on the following components: underside of the cover, deflectors, transport tube, transition section, impactor stage, impactor plate, filter top assembly, and afterfilter.

## 6.2 INLET PERFORMANCE WITH FLOW DEFLECTORS IN PLACE

Table 14 presents results of the mass balance tests conducted at a wind speed of 2 km/hr. For this single test, aspiration efficiency of the RAAMP sampler was measured to be approximately 96% and overall sampler effectiveness measured 62%. As shown in Table 15, fractional losses of particles to the transport tube and transition section were negligible. It is interesting to note that particle losses to the impactor stage (9.6% by mass) were considerably lower than the 18.4% value measured previously using the 7.6 cm diameter transport tube. It is also of interest that the impactor stage efficiency decreased from 17.7% to 11.4%. These changes in impactor stage losses and impactor stage efficiency are clearly due to the difference between the two transport tube designs. In the original design, the transport tube had a circular cross-section of 7.6 cm diameter resulting in a mean transport velocity of 432 cm/sec. In the modified design, the transport tube has a rectangular cross-section of 17 cm x 11.5 cm resulting in a mean transport velocity of 99 cm/sec. This dramatic reduction in transport velocity results in reduced particle losses to the top of the impactor stage. The fact that the newer transport tube more uniformly distributes the aerosol towards the stage's impaction jets probably accounts for the noted decrease in impactor stage efficiency. Non-uniform flow through the stage's parallel plates would tend to increase the stage's efficiency. The manufacturer's observations of collected mass deposits during field evaluation of the modified sampler tend to support this hypothesis. As a final note regarding the 2 km/hr test results, no significant change in filter top assembly losses nor filter penetration values were observed during evaluation of the modified components.

Tables 14 and 15 also summarize test results obtained during wind tunnel evaluation of the modified components at a wind speed of 24 km/hr. Similar to the 2 km/hr tests, sampler aspiration at 24 km/hr was near 100%. However, the overall 16.4% effectiveness of the sampler at this wind speed was a considerable decrease from the 62% value measured at 2 km/hr. Unlike the 2 km/hr performance tests, losses to the sampler's cap, deflector, transport tube, and impactor stage were all significant at 24 km/hr and accounted for nearly 50% of the aspirated aerosol mass. It is of particular interest to note that the impactor stage losses, filter top assembly losses, and impactor stage efficiency all dramatically increased at the higher wind speed. It is hypothesized

that the large dimensions and relatively short transport distance of the rectangular transport tube may result in conservation of the approaching wind speed through the transport tube. If this were the case, the downward velocity through the transport tube would more closely match that of the freestream than that calculated simply by dividing the flowrate by the transport tube's cross-sectional area. A higher velocity in this section would account for the observed increase in particle losses and impactor stage efficiency.

### **6.3 INLET PERFORMANCE WITHOUT FLOW DEFLECTORS**

In an effort to gain a better understanding of the effect inlet geometry has on overall sampler performance, a single mass balance test was conducted following the removal of the flow deflectors from the rectangular inlet. For comparison purposes, this test was conducted using liquid test aerosols of 10 micrometers aerodynamic diameter in conjunction with a tunnel wind speed of 24 km/hr. As summarized in Table 16, the most significant effect of this modification was the observed reduction in sampler aspiration efficiency from 105% to 56%. In the absence of the flow deflectors, the low suction velocity of the rectangular inlet (relative to the freestream velocity) is insufficient to capture a representative fraction of the challenge aerosol. This reduction in aspiration efficiency is the primary reason for the noted decrease in overall effectiveness from 16.4% to 9.4%. Table 16 summarizes fractional particle losses associated with each of the sampler's components for this test condition. In general, removal of the flow deflector resulted in no significant change in transport tube losses, transition section losses, impactor stage losses, filter top assembly losses, impactor efficiency, or filter penetration.

## 7.0 SUMMARY AND RECOMMENDATIONS

As an integral part of this Phase 1 project, the EPA-AREAL wind tunnel has been fully characterized at wind speeds of 2 km/hr and 24 km/hr using test aerosols of 10 micrometers aerodynamic diameter. At these wind speeds, the facility and its operating protocol currently met or exceeded all 40 CFR Part 53 acceptance criteria regarding PM10 size-selective performance evaluation. These acceptance criteria relate to mean velocity and velocity uniformity in the test section, aerosol generation procedures and aerosol quality, and the spatial uniformity of test aerosols in the test section. Analytical procedures for accurate quantitation of collected mass deposits also met 40 CFR Part 53 criteria. Recent revisions in test procedure and recent modifications to the wind tunnel have been shown to be of value towards providing more reliable wind tunnel test results.

The RAAMP sampler was received in good condition from its manufacturer and all critical components were found to be operational. Flow calibration of the RAAMP sampler showed that the actual volumetric flowrate was approximately 4% higher than the 1.13 m<sup>3</sup>/min design value but could be accurately predicted using look-up tables provided by the flow controller's manufacturer.

Wind tunnel performance tests of the RAAMP sampler were conducted using liquid test aerosols of 10 micrometers aerodynamic diameter. For this particle size of the greatest interest, the sampler's overall effectiveness was measured to be 29% and 14% at wind speeds of 2 km/hr and 24 km/hr, respectively. Extensive mass balance tests of the sampler revealed that the close proximity of the instrument case to the sampling inlet was artificially enriching the sampled concentration resulting in measured aspiration efficiencies of approximately 115% at both tested wind speeds. Because the sampling inlet is not centered over the instrument case, aspiration efficiency was also expected to be a function of wind direction relative to the sampler. Modifications were made to the experimental setup to remove the adverse influence of the housing and resulted in measured aspiration efficiencies near 100% independent of wind speed.

Particle losses to the inlet screen were found to be excessive at both wind speeds and partially accounted for the sampler's low overall performance. While losses to the inlet head and inlet tube were found to be acceptable at a wind speed of 2 km/hr, performance tests at 24 km/hr revealed that losses to these components were prohibitively high. In fact, the sampler's lower overall effectiveness at 24 km/hr compared to 2 km/hr can be attributed primarily to increased transport losses to the screen, inlet head, and inlet tube rather than differences in sampler aspiration efficiency. Fractional losses to the impactor stage were found to be approximately 26% independent of wind speed.

As expected, the performance of the RAAMP sampler's size fractionation section was generally found to be independent of wind speed or inlet flow configuration. Test results suggest that this section was performing approximately as intended with an average stage penetration value of close to 50% for 10 micrometer aerodynamic aerosols.

In view of these test results, the manufacturer of the RAAMP sampler made some design changes to key components of the sampler which included the sampler's impaction stage, transition section, and main inlet. To evaluate the individual contribution of the component changes on overall sampler performance, these modified components were evaluated during separate wind tunnel tests.

Mass balance tests conducted with the modified impaction plate in place indicated a fairly significant increase in sampler effectiveness from 34% to 59% at a tunnel wind speed of 2 km/hr. Analysis of test results revealed that this effectiveness increase was partly due to lowered impaction stage losses. The majority of the noted increased effectiveness, however, was a dramatic decrease in impaction stage fractional efficiency from 41% to 18%. Tapering of the jet entries to reduce stage losses also adversely affected the stage performance accounting for the observed penetration through the stage.

The addition of the modified transition (in tandem with the modified impactor stage) resulted in an overall sampler effectiveness of 44%. Altering the geometry of the transition section resulted in alteration of the flow distribution through the impaction stage. Modification of the flow distribution through the impaction stage resulted in slightly higher stage fractional efficiency accounting for the observed reduction in sampler effectiveness.

Test results with the original inlet of the RAAMP sampler revealed that the inlet's aspiration characteristics were acceptable but that losses to the inlet's screen and internal surfaces were unacceptably high. In an effort to minimize these losses, the inlet and transport tube of the RAAMP sampler were redesigned. Wind tunnel tests were then conducted with the modified inlet in conjunction with the modified impactor stage and modified transition section. Similar to the tests conducted with the original RAAMP inlet, aspiration efficiencies of 10  $\mu\text{m}$  test aerosols with the modified inlet approached 100%. However, particle losses to the sampler's cap, deflector, transport tube, and impactor stage were all significant at 24 km/hr and resulted in a sampler effectiveness of 16% compared to the 62% value measured during the 2 km/hr tests. Removal of the flow deflectors reduced sampler aspiration efficiency to approximately 56% resulting in an overall effectiveness of 9%. Removal of the flow deflectors resulted in no significant change in transport tube losses, transition section losses, impactor stage losses, filter top assembly losses, or impactor efficiency.

Based on these test results, the following recommendations are made regarding future development of the RAAMP sampler:

- 1) The adverse influence of the instrument case on the flow field around the sampling needs to be addressed and can best be corrected by extending the inlet to an elevation at least 75 cm from the top of the case. Flow visualization around the modified inlet will aid in selecting the optimal height above the case. As predicted by empirical relationships, turbulent deposition losses in this increased length of transport tube are expected to be negligible.
- 2) Particle losses to the sampler's inlet screen are prohibitive even at a wind speed of 2 km/hr and the screen should be redesigned to minimize particle losses while still preventing intrusion by large flying insects into the sampler. Reduced particle losses can be expected by using a screen with both greater fractional open area and thicker wires than exist in the current design.
- 3) Particle losses to the inlet head and transport tube are excessive especially at wind speeds of 24 km/hr. In the current design, the incoming airstream must undergo three separate right-angle turns prior to entering the sampler's transport section. To minimize entry losses, the inlet should be redesigned to require a single 90° transition from the airstream's direction to that of the vertical transport tube. Since isotopic analysis of collected large particles is also of interest to the sampler's manufacturer, this inlet configuration will also maximize the collection and subsequent transport of particles larger than 10 micrometer diameter.
- 4) Particle losses to the sampler's current impactor stage will also need to be reduced as part of the sampler redesign. It is first recommended that the transition from the transport tube to the impaction stage region be expanded to reduce turbulent inertial losses on the top of the plate. It is also recommended that the stage's sharp-edged impactor jets be tapered at their inlets to reduce entry losses and interjet losses. Since the current throat length to jet width (T/W) of the jets is only approximately equal to unity in its current configuration, the thickness of the impactor stage may need to be increased to ensure that particles entering the jet have sufficient residence time to be accelerated to the jet velocity.
- 5) Losses to the underside of the impactor stage can probably be reduced to an acceptable value by increasing the current jet to plate distance by a factor of two until an S/W value of at least three is achieved. Consideration should also be given to increasing the existing distance between impactor nozzles as intrajet interference may be responsible for turbulent deposition on the underside of the impactor plate.

- 6) Approximately 18% of the aerosol not collected by the impactor plate is currently lost in the region upstream of the sampler's afterfilter. Modifying the geometry in this region may lead to acceptable fractional losses. The overall characteristics of the sampler's size fractionation components appear to be acceptable, however, and may not require further attention during the sampler's redesign.
- 7) Should funding and logistical constraints preclude a full redesign and evaluation of the RAAMP sampler, it is recommended that the existing field samplers be modified by extending the inlet to an elevation at least 75 from the top of the case. This modification could be performed at minimal cost and should minimize the adverse effect of the instrument case on the sampler's aspiration characteristics. To maximize overall particle collection, it is also recommended that the inlet screen of existing samplers be removed from the inlet.

If further development of the RAAMP sampler appears unlikely, it is also recommended that the existing sampler be fully characterized in the wind tunnel using solid aerosols. Because the nature of solid aerosols better represents the composition of atmospheric aerosols, use of solid calibration aerosols would provide a more accurate measure of the sampler's field performance than would the use of liquid calibration aerosols. In particular, it is expected that solid calibration aerosols would experience less internal losses than would liquid calibration aerosols of the same diameter. At a minimum, it is suggested that mass balance tests be conducted using solid calibration aerosols of 3, 5, 7, 9, 10, 11, 13, 15, and 20  $\mu\text{m}$  aerodynamic diameter in conjunction with wind speeds of 2 km/hr and 24 km/hr. Solid calibration aerosols up to 50  $\mu\text{m}$  aerodynamic diameter would be used to determine the RAAMP sampler's ability to efficiently capture large particles from the atmosphere and effectively transport them to the impaction plate for subsequent quantitation.

## 8.0 REFERENCES

- Golovin, M.N. and A.A. Putnam. (1962). "Inertial Impaction on Single Elements." Ind. Engng. Chem. Fundls., Vol. 1, pp. 264-273.
- Hangal, S. and K. Willeke. (1990). "Overall Efficiency of Tubular Inlets Sampling at 0-90 Degrees from Horizontal Aerosol Flows." Atmos. Environ., Vol. 24A(9), pp. 2370-2386.
- Liu, B.Y.H. and J.K. Agarwal. (1974). "Experimental Observation of Aerosol Deposition in Turbulent Flow." J. Aerosol Sci., Vol. 5, pp. 145-155.
- Marple, V.A. and K. Willeke. (1976). "Impactor Design." Atmos. Environ., Vol. 12, pp. 891-896.
- Olan-Figueroa, E., McFarland, A.R., and C.A. Ortiz. (1982). "Flattening Coefficients for DOP and Oleic Acid Droplets Deposited on Treated Glass Slides." AIHA Journal, Vol. 43, pp. 395-399.

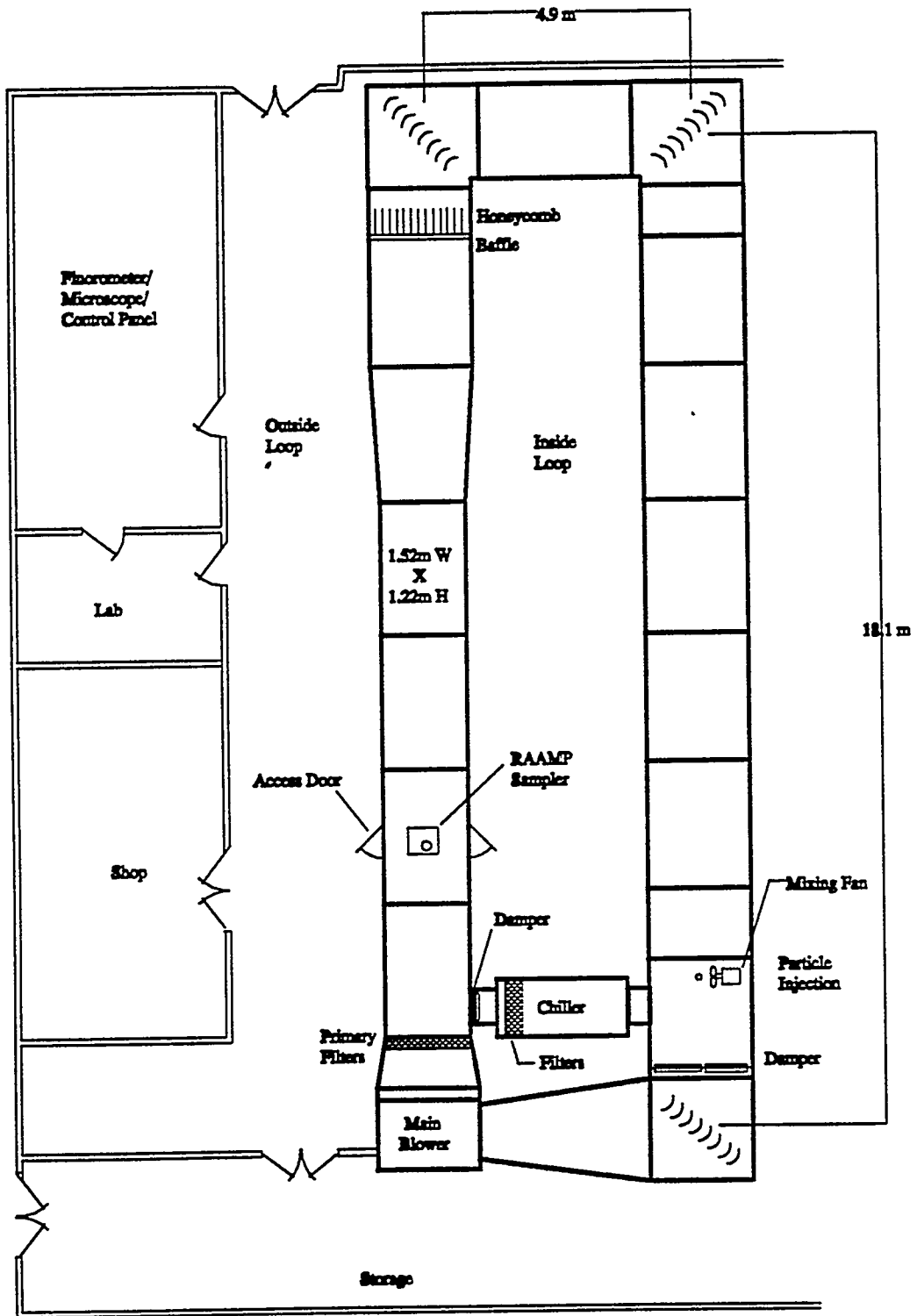


Figure 1. Plan view of the EPA-AREAL Aerosol Test Facility

View:  
Looking Towards  
Main Blower

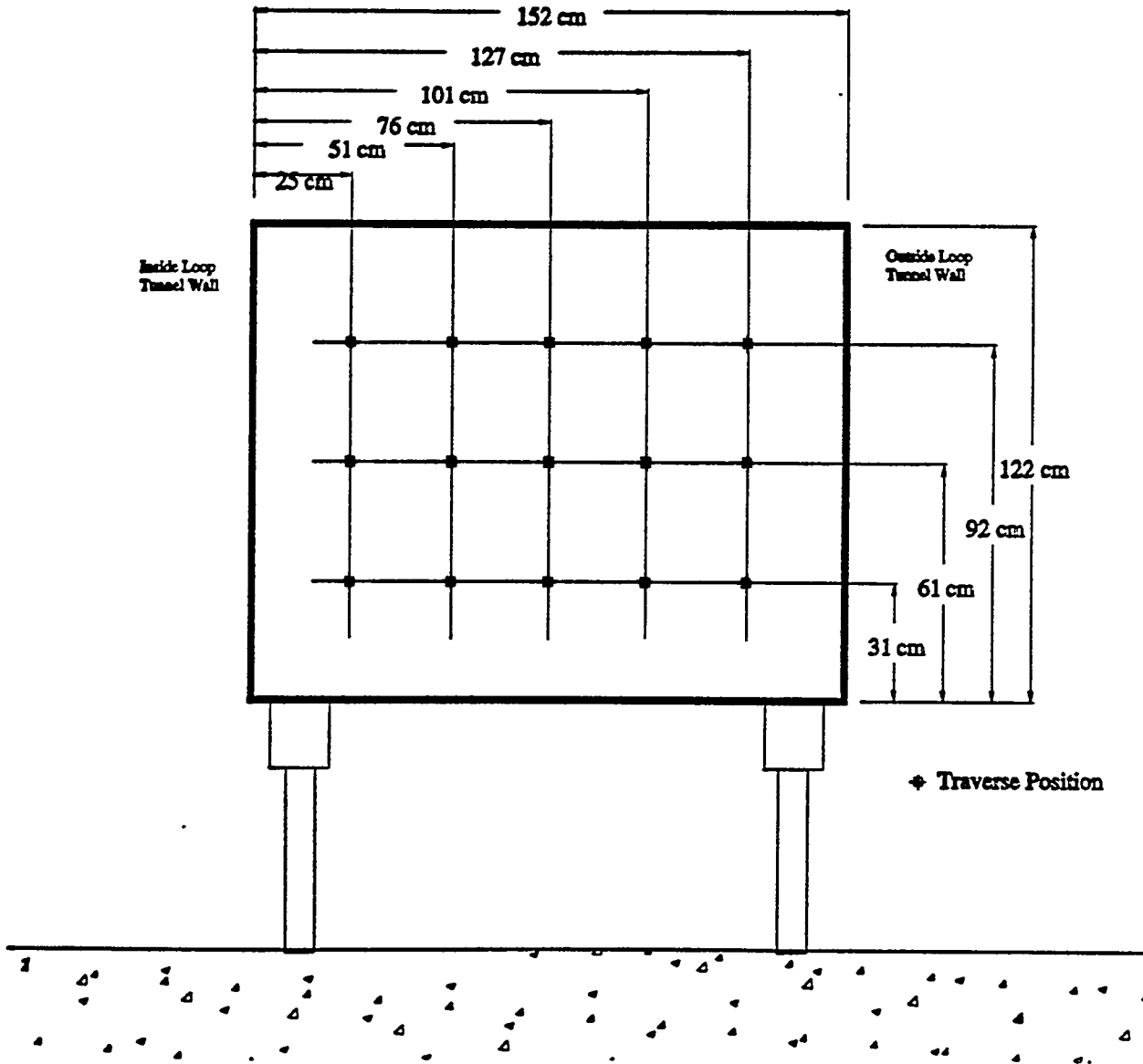


Figure 2. Schematic of the wind tunnel test section showing location of velocity traverse points.

**2 Km/hr Baffle**

**View: Looking Towards  
Honeycomb**

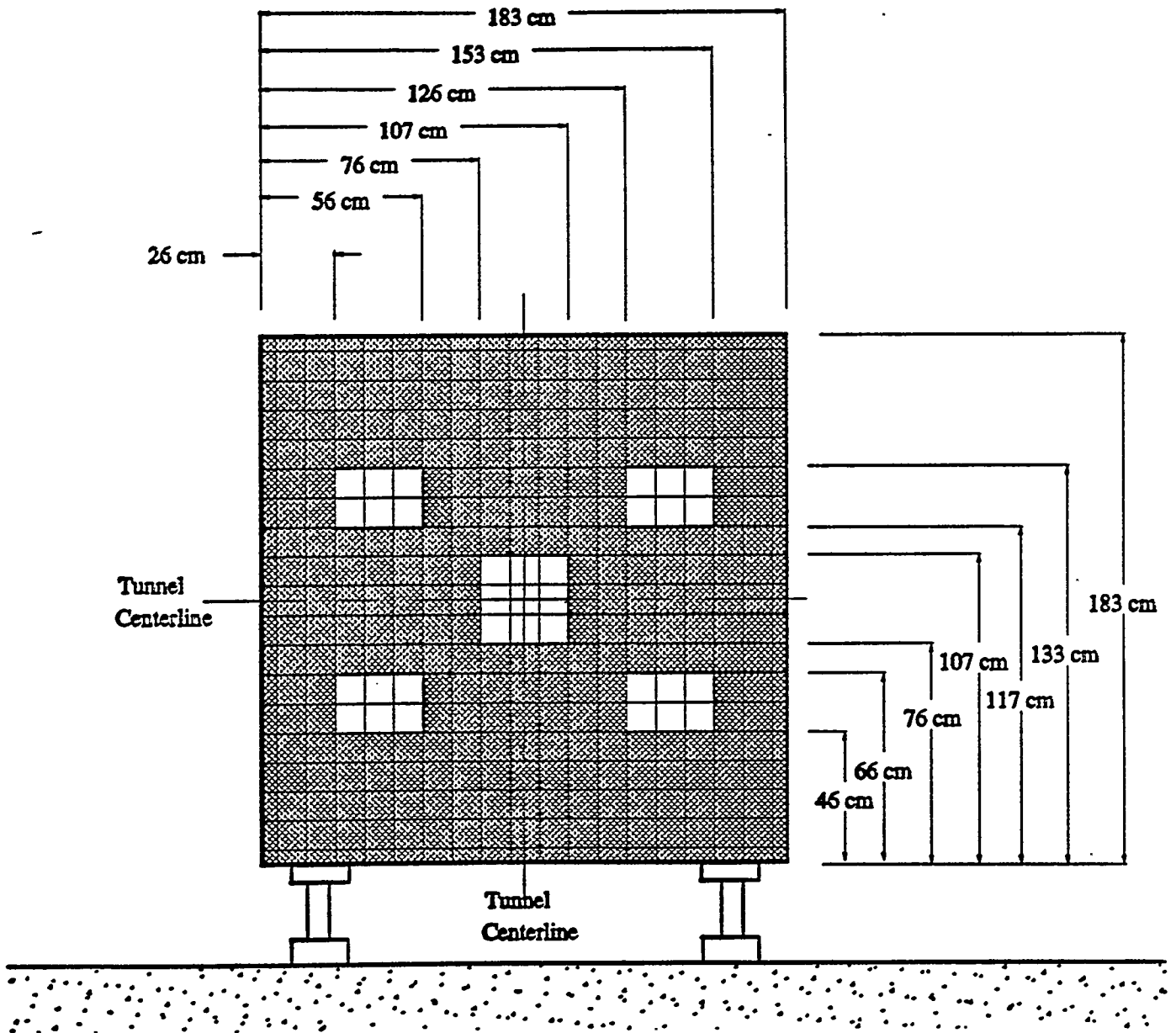


Figure 3. Critical dimensions of the baffle used during the 2 km/hr wind tunnel tests.

**24 Km/hr Baffle**

**View: Looking Towards  
Honeycomb**

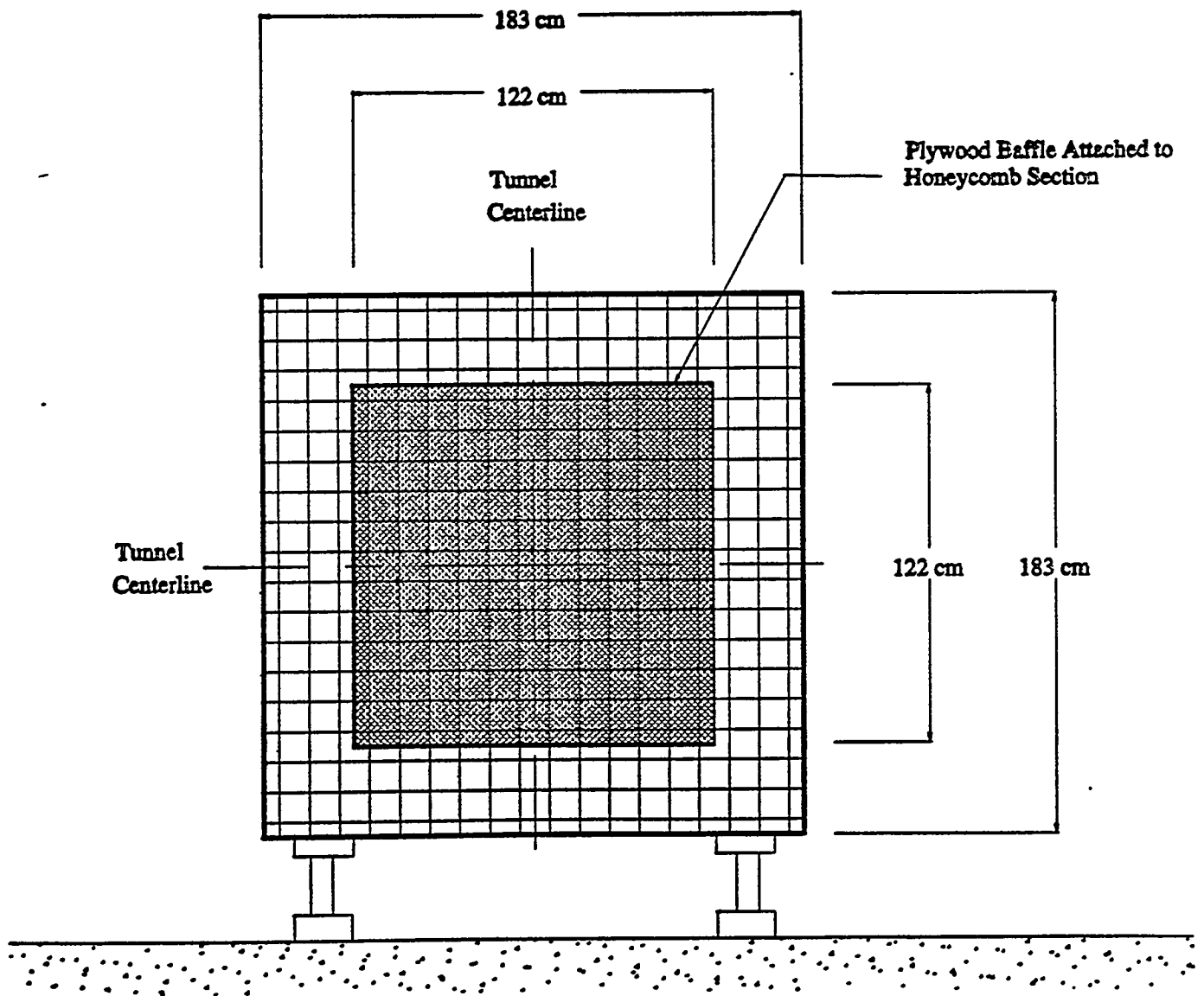


Figure 4. Critical dimensions of the baffle used during the 24 km/hr wind tunnel tests.

**View of Test Section  
Looking Towards  
Main Blower**

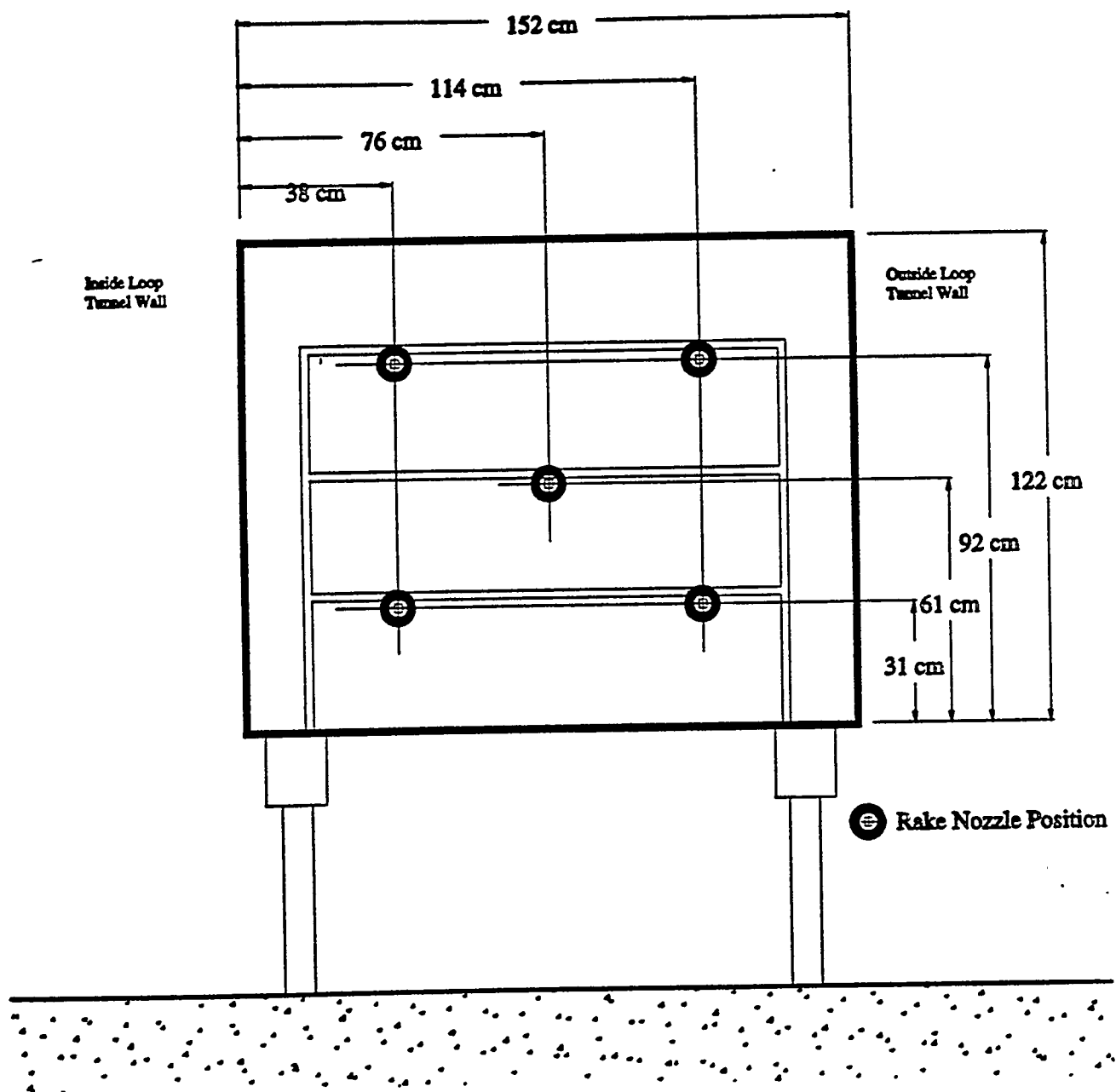


Figure 5. Critical dimensions of the RAKE sampler showing locations of aerosol sampling points.

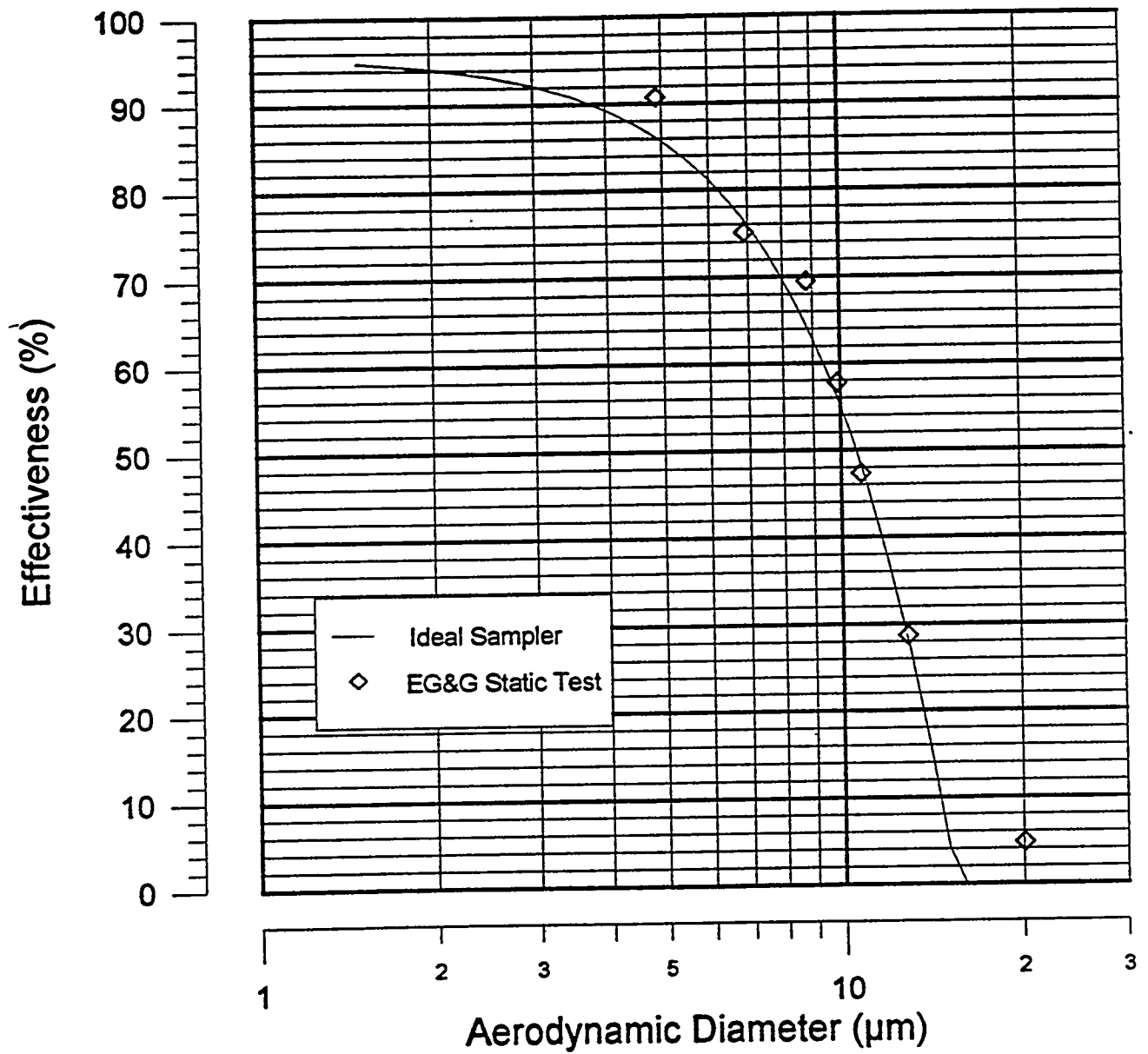


Figure 6. Performance of the EG&G sampler under static test conditions.

View Looking at  
Test Section from  
Above

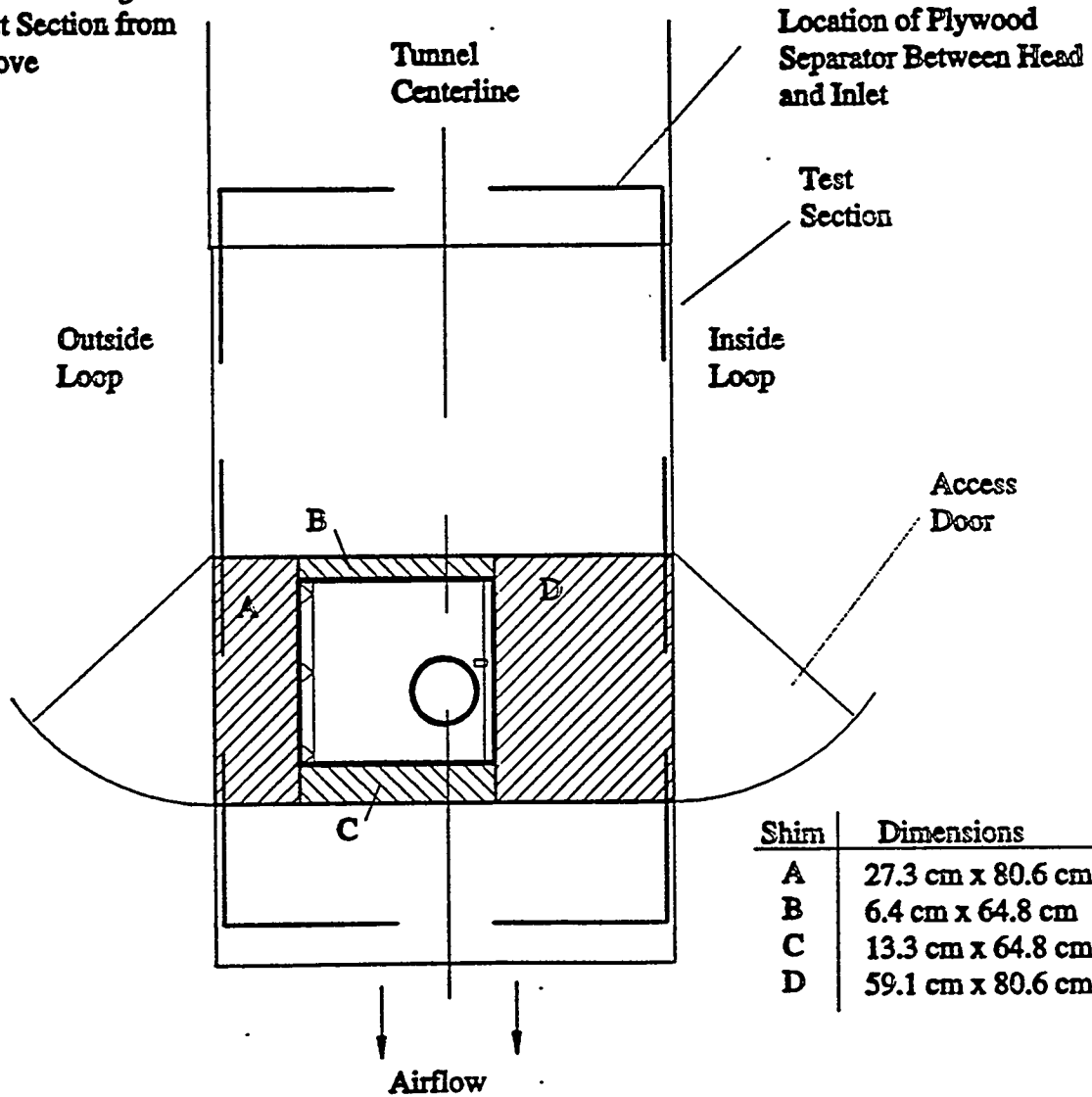


Figure 7. Plan view of the wind tunnel test section showing the EG&G sampler location during performance tests.

**View of RAAMP Sampler in  
Test Section Looking  
Towards Blower**

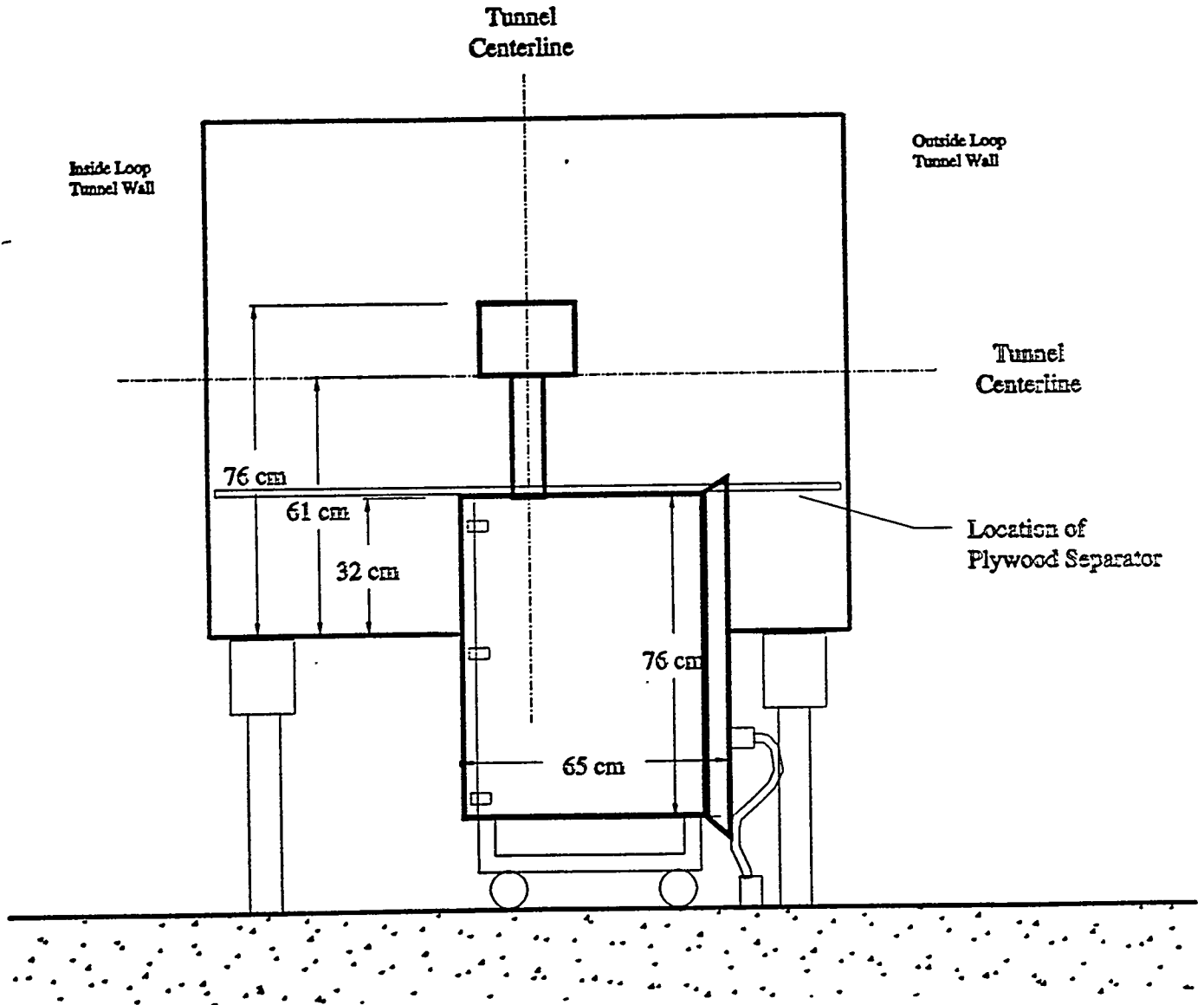


Figure 8. Side view of the EG&G sampler showing its location in the test section during wind tunnel evaluation.

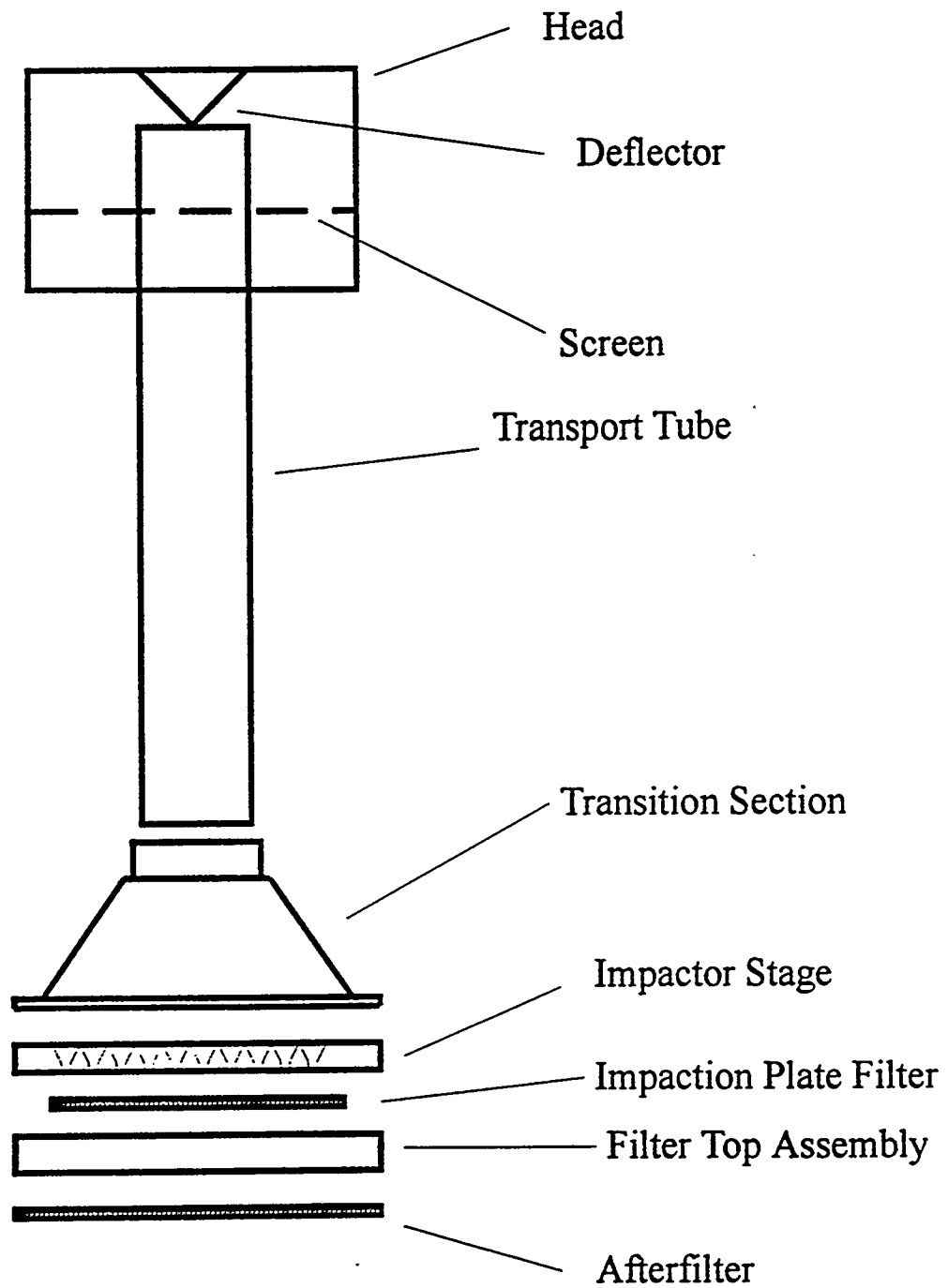


Figure 9. Schematic of the RAAMP sampler showing components involved in the mass balance tests.

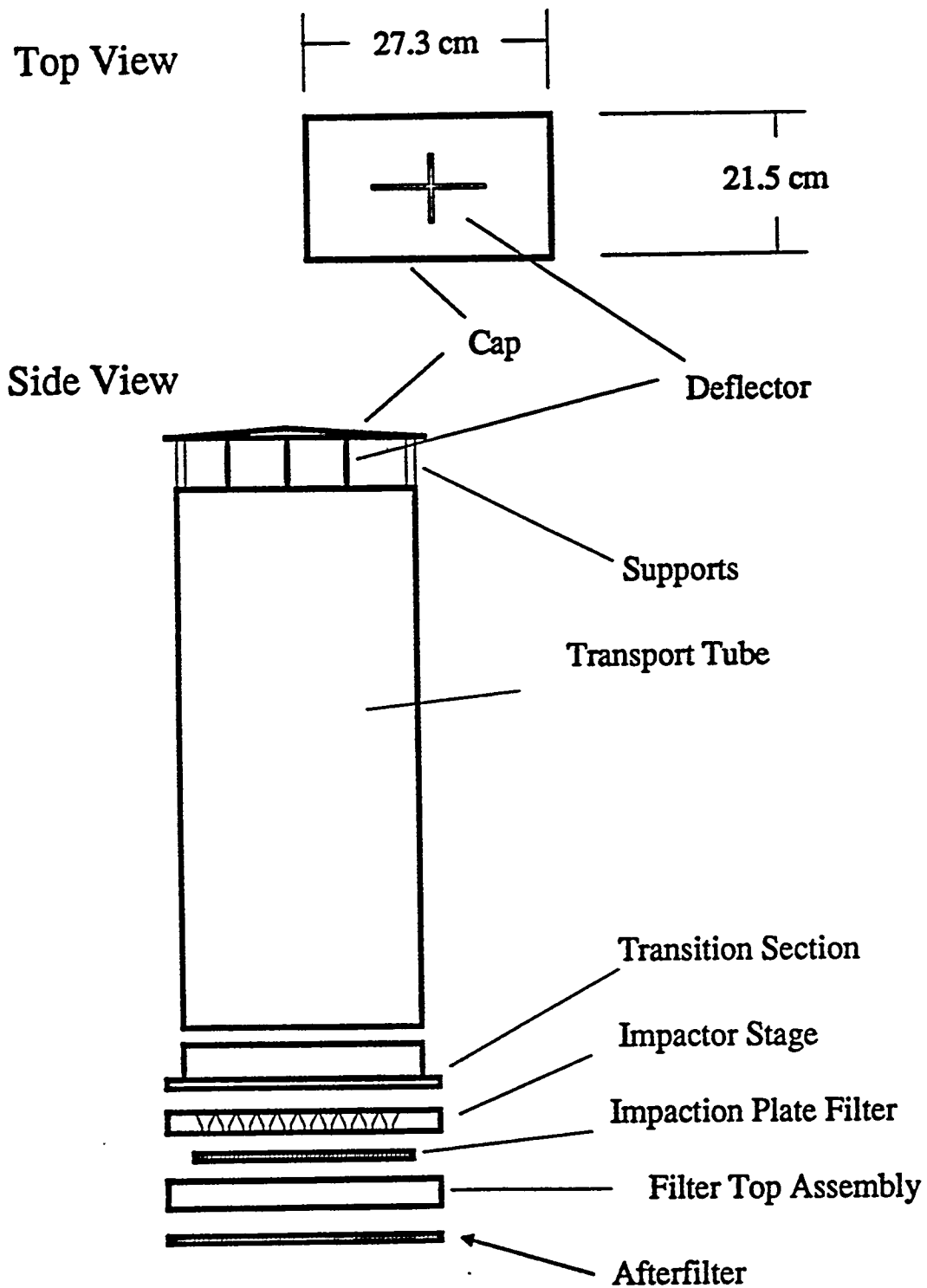


Figure 10. Schematic of the modified RAAMP sampler showing components involved in the mass balance tests.

Table 1. Velocity profile of EPA Aerosol Test Facility at 2 Km/hr test wind speed.

Vertical Position from Tunnel Floor	Horizontal Position from Inside Loop Wall					
	25 cm	51 cm	76 cm	101 cm	127 cm	
92 cm	2.09 0.29 14 103	NM	2.09 0.32 15 103	NM	2.09 0.32 15 103	Mean Velocity <sup>1</sup> , Km/hr RMS Velocity <sup>1</sup> , Km/hr Turbulence Intensity <sup>2</sup> , % % Dev of Avg Vel <sup>3</sup> , %
61 cm	2.02 0.32 16 100	NM	1.98 0.32 16 98	NM	2.05 0.32 16 101	Mean Velocity, Km/hr RMS Velocity, Km/hr Turbulence Intensity, % % Dev of Avg Vel, %
32 cm	1.98 0.32 16 98	NM	1.94 0.32 16 96	NM	1.98 0.29 15 98	Mean Velocity, Km/hr RMS Velocity, Km/hr Turbulence Intensity, % % Dev of Avg Vel, %
Statistics:						
Average Mean Velocity		2.02 Km/hr				
Percent of 2 Km/hr goal		101%				
Tunnel Conditions:						
Date:		30 JUN 1994				
Large Blower:		OFF Damper in full closed position				
Bypass Chiller:		ON Chilled water slightly on to maintain tunnel temp at 21°C Damper open slightly greater than 1/2				
Filters:		Bag filters in main loop Bag filters and HEPA in bypass loop				
Baffles:		5 hole baffle in place attached to downstream side of honeycomb section				

NM = Not Measured

<sup>1</sup> Mean Velocity and RMS Velocity were measured with a single-wire, fiber-film probe operated with a sampling frequency of 0.05 KHz.

<sup>2</sup> Turbulence Intensity = RMS Velocity / Mean Velocity \* 100%.

<sup>3</sup> % Dev of Avg Vel = Mean Velocity (at each point) / Average Mean Velocity \* 100%.

Table 2. Velocity profile of EPA Aerosol Test Facility at 24 Km/hr test wind speed.

Vertical Position from Tunnel Floor	Horizontal Position from Inside Loop Wall					
	25 cm	51 cm	76 cm	101 cm	127 cm	
92 cm	24.5	24.1	23.2	23.4	24.5	Mean Velocity <sup>1</sup> , Km/hr RMS Velocity <sup>1</sup> , Km/hr Turbulence Intensity <sup>2</sup> , % % Dev of Avg Vel <sup>3</sup> , %
	1.4	1.4	1.4	1.4	1.4	
	5.9	6.0	6.2	6.2	5.9	
	103	102	99	99	103	
61 cm	23.8	23.8	23.4	23.4	23.4	Mean Velocity, Km/hr RMS Velocity, Km/hr Turbulence Intensity, % % Dev of Avg Vel, %
	1.4	1.4	1.4	1.4	1.4	
	6.1	6.1	6.2	6.2	6.2	
	100	100	99	99	99	
32 cm	23.8	23.8	23.4	23.4	23.4	Mean Velocity, Km/hr RMS Velocity, Km/hr Turbulence Intensity, % % Dev of Avg Vel, %
	1.4	1.4	1.1	1.1	1.4	
	6.1	6.1	4.6	4.6	6.2	
	100	100	99	99	99	
Statistics:						
Average Mean Velocity		23.7 Km/hr				
Percent of 24 Km/hr goal		99%				
Tunnel Conditions:						
Date:		13 MAY 1994				
Large Blower:		ON - Pot Setting = 157 Damper in full open position				
Bypass Chiller:		ON Chilled water full open to maintain tunnel temp at 21°C Damper full open				
Filters:		Bag filters in main loop Bag filters and HEPA in bypass loop				
Baffles:		4 ft by 4 ft baffle in place attached to downstream side of honeycomb section				

NM = Not Measured

<sup>1</sup> Mean Velocity and RMS Velocity were measured with a single-wire, fiber-film probe operated with a sampling frequency of 0.05 KHz.

<sup>2</sup> Turbulence Intensity = RMS Velocity / Mean Velocity \* 100%.

<sup>3</sup> % Dev of Avg Vel = Mean Velocity (at each point) / Average Mean Velocity \* 100%.

Table 3. Typical uniformity of 10 µm aerosol at a wind speed of 2 Km/hr.

Vertical Position from Tunnel Floor	Horizontal Position from Inside Loop Wall			
	38 cm	76 cm	114 cm	
92 cm	2 1.61 98		6 1.68 102	Rake Position No. Uranine Conc, µg/m <sup>3</sup> Percent of Avg Conc, %
61 cm		4 1.69 102		Rake Position No. Uranine Conc, µg/m <sup>3</sup> Percent of Avg Conc, %
32 cm	3 1.59 96		5 1.67 101	Rake Position No. Uranine Conc, µg/m <sup>3</sup> Percent of Avg Conc, %
Statistics: Average Uranine Conc. Coefficient of Variation		1.65 µg/m <sup>3</sup> 2.6 %		
Tunnel Conditions:		Date: 30 JUN 1994 Large Blower: OFF Damper in full closed position Bypass Chiller: ON Chilled water slightly on to maintain tunnel temp at 21°C Damper open slightly greater than 1/2 Filters: Bag filters in main loop Bag filters and HEPA in bypass loop Baffles: 5 hole baffle in place attached to downstream side of honeycomb section		

Table 4. Typical uniformity of 10 µm aerosol at a wind speed of 24 Km/hr.

Vertical Position from Tunnel Floor	Horizontal Position from Inside Loop Wall			
	38 cm	76 cm	114 cm	
92 cm	2 0.164 105		6 0.147 94	Rake Position No. Uranine Conc, µg/m <sup>3</sup> Percent of Avg Conc, %
61 cm		4 0.156 100		Rake Position No. Uranine Conc, µg/m <sup>3</sup> Percent of Avg Conc, %
32 cm	3 0.161 103		5 0.150 96	Rake Position No. Uranine Conc, µg/m <sup>3</sup> Percent of Avg Conc, %
Statistics:				
Average Uranine Conc.		0.156 µg/m <sup>3</sup>		
Coefficient of Variation		4.6 %		
Tunnel Conditions:				
Date:		8 JUN 1994		
Large Blower:		ON - Pot Setting = 157 Damper in full open position		
Bypass Chiller:		ON Chilled water full open to maintain tunnel temp at 21°C Damper full open		
Filters:		Bag filters in main loop Bag filters and HEPA in bypass loop		
Baffles:		4 ft by 4 ft baffle in place attached to downstream side of honeycomb section		

**Table 5. Total fluorometric mass collected on blank filters, tunnel background, and during 10 µm aerosol generation.**

		Total Fluorometric Mass (ng)	
		2 Km/hr	24 Km/hr
<b>8" X 10" Glass Filter Blanks</b>		<b>9,5,7</b>	<b>9,5,7</b>
<b>Tunnel Background</b>		<b>9 (filter) + 5 (nozzle)</b>	<b>12 (filter) + 9 (nozzle)</b>
<b>ISO Runs:</b>			
	Run 1	55,288 (30 min)	11,571 (60 min)
	Run 2	56,256 ( " )	12,550 ( " )
	Run 3	56,436 ( " )	12,213 ( " )
	Run 4	54,079 ( " )	
	Run 5	54,779 ( " )	
<b>Statistics:</b>			
	Mean =	55,368	12,111
	CV =	1.8%	4.1%

Table 6. Total fluorometric mass measured on 47-mm filter blanks compared with the RAKE filters collected at 24 km/hr and during 10  $\mu$ m aerosol generation.

Filter Number	Total Fluorometric Mass (ng)	
	47-mm filter blanks	24 Km/hr RAKE filters
1	0.2	466
2	0.6	541
3	0.4	475
4	0.4	495
5	0.3	452
6	0.7	
7	0.4	
8	0.2	
9	0.2	
10	0.8	
Statistics:	Mean = 0.4 CV = 50%	

Table 7. Flow calibration performed on the RAAMP sampler.

	Test 1	Test 2
Calibration Date	11 MAY 1994	10 JUN 1994
Ambient Pressure, mmHg	758	757
Ambient Temperature, °C	22.0	22.5
Measured Flow <sup>1</sup> , actual m <sup>3</sup> /min	1.174	1.181
Look-up Table Flow, actual m <sup>3</sup> /min	1.165	1.167
Relative Error <sup>2</sup>	+0.8	+1.2

<sup>1</sup> Measured Flow determined with Graseby-Andersen orifice meter.

<sup>2</sup> Relative Error = (Measured Flow - Look-up Table Flow) / Measured Flow.

Table 8. RAAMP sampler wash test results for 2 km/hr and 10 µm aerosol.

Sampler Component	Inlet and Body in Wind Tunnel		Inlet Separated from Body		Inlet Separated from Body - Screen Removed	
	Uranine Conc µg/m <sup>3</sup>	Percent of Mass %	Uranine Conc µg/m <sup>3</sup>	Percent of Mass %	Uranine Conc µg/m <sup>3</sup>	Percent of Mass %
Head	0.002	0	0.001	0	0.001	0
Screen	0.283	14	0.163	10	NA	NA
Tube	0.054	3	0.037	2	0.055	3
Expansion	0.040	2	0.026	2	0.022	1
Impactor Stage	0.498	25	0.340	22	0.396	25
Impactor Plate	0.430	22	0.388	25	0.487	31
Filter Assembly Top	0.167	8	0.120	8	0.072	4
Afterfilter	0.501	31	0.486	31	0.555	35
Sum =	1.980		1.561		1.588	
Tunnel Concentration <sup>1</sup>	1.720		1.605		1.630	
Aspiration Efficiency <sup>2</sup>	115%		97%		97%	
Percent Effectiveness <sup>3</sup>	29%		30%		34%	

NA = Not applicable

<sup>1</sup> Tunnel Conc determined using the isokinetic high volume ISO sampler.

<sup>2</sup> Aspiration Efficiency = total sampler collected mass concentration (Sum) divided by the Tunnel Conc.

<sup>3</sup> Percent Effectiveness = Afterfilter mass concentration divided by the Tunnel Conc.

Table 9. RAAMP sampler wash test results for 24 km/hr and 10 µm aerosol.

Sampler Component	Inlet and Body in Wind Tunnel		Inlet Separated from Body		Inlet Separated from Body - Screen Removed	
	Uranine Conc µg/m <sup>3</sup>	Percent of Mass %	Uranine Conc µg/m <sup>3</sup>	Percent of Mass %	Uranine Conc µg/m <sup>3</sup>	Percent of Mass %
Head	0.043	19	0.032	18	0.043	26
Screen	0.104	45	0.076	43	NA	NA
Tube	0.006	3	0.005	3	0.018	11
Expansion	0.002	1	0.001	1	0.002	1
Impactor Stage	0.020	9	0.015	8	0.025	15
Impactor Plate	0.022	10	0.019	11	0.029	18
Filter Assembly Top	0.006	3	0.006	3	0.008	5
Afterfilter	0.027	12	0.024	13	0.037	23
Sum =	0.230		0.178		0.162	
Tunnel Concentration <sup>1</sup>	0.196		0.178		0.172	
Aspiration Efficiency <sup>2</sup>	117%		100%		94%	
Percent Effectiveness <sup>3</sup>	14%		13%		23%	

NA = Not applicable

- <sup>1</sup> Tunnel Conc determined using the isokinetic high volume ISO sampler.
- <sup>2</sup> Aspiration Efficiency = total sampler collected mass concentration (Sum) divided by the Tunnel Conc.
- <sup>3</sup> Percent Effectiveness = Afterfilter mass concentration divided by the Tunnel Conc.

Table 10. Particle transport losses attributed to individual RAAMP sampler components.

	Transport Tube Losses <sup>1</sup> (%)		Transition Section Losses <sup>2</sup> (%)		Impactor Stage Losses <sup>3</sup> (%)		Filter Top Assembly Losses <sup>4</sup> (%)	
	2 Km/hr	24 Km/hr	2 Km/hr	24 Km/hr	2 Km/hr	24 Km/hr	2 Km/hr	24 Km/hr
Inlet and Body	4	8	2	3	31	26	24	13
Inlet Only with Screen	2	8	2	3	26	23	21	19
Inlet Only without Screen	3	15	1	2	26	25	10	18
Statistics: Mean (%) CV	7 0.69		2 0.34		26 0.10		18 0.30	

<sup>1</sup> Transport Tube Losses = transport tube mass / (mass collected on transport tube + transition section + impactor stage + impaction plate + filter assembly + afterfilter).

<sup>2</sup> Transition Section Losses = transition section mass / (mass collected on transition section + impactor stage + impaction plate + filter assembly + afterfilter).

<sup>3</sup> Impactor Stage Losses = impactor stage mass / (mass collected on impactor stage + impaction plate + filter assembly + afterfilter).

<sup>4</sup> Filter Top Assembly Losses = filter top assembly mass / (mass collected on filter top assembly + afterfilter mass).

Table 11. Characteristics of the RAAMP sampler's size fractionation components.

	Impactor Efficiency <sup>1</sup> (%)		Filter Penetration <sup>2</sup> (%)	
	2 Km/hr	24 Km/hr	2 Km/hr	24 Km/hr
Inlet and Body	40	40	45	48
Inlet Only with Screen	39	41	48	48
Inlet Only without Screen	44	39	50	50
Statistics: Mean (%) CV	40 0.046		48 0.038	

<sup>1</sup> Impactor Efficiency = impactor plate mass / (mass collected on impactor plate + filter assembly + afterfilter).

<sup>2</sup> Filter Penetration = after filter mass / (mass collected on impactor plate + filter assembly + afterfilter).

Table 12. RAAMP sampler wash test results for 2 km/hr and 10 µm aerosol with the angled impactor stage installed (inlet separated from body with screen removed).

Sampler Component	Original Transition Section Installed		New Transition Section Installed	
	Uranine Conc µg/m <sup>3</sup>	Percent of Mass %	Uranine Conc µg/m <sup>3</sup>	Percent of Mass %
Head	0.001	0	0.000	0
Screen	NA	NA	NA	NA
Tube	0.008	1	0.050	3
Original Transition	0.005	0	NA	NA
New Transition	NA	NA	0.052	3
Impactor Stage	0.298	17	0.260	17
Impactor Plate	0.258	15	0.278	18
Filter Assembly Top	0.192	11	0.154	10
Afterfilter	1.008	57	0.722	48
Sum =	1.767		1.516	
Tunnel Concentration <sup>1</sup>	1.714		1.640	
Aspiration Efficiency <sup>2</sup>	103%		92%	
Percent Effectiveness <sup>3</sup>	59%		44%	

NA = Not applicable

- <sup>1</sup> Tunnel Conc determined using the isokinetic high volume ISO sampler.
- <sup>2</sup> Aspiration Efficiency = total sampler collected mass concentration (Sum) divided by the Tunnel Conc.
- <sup>3</sup> Percent Effectiveness = Afterfilter mass concentration divided by the Tunnel Conc.

**Table 13.** Particle transport losses attributed to individual components and characteristics of size fractionation components of the RAAMP sampler at a wind speed of 2 km/hr and 10  $\mu$ m aerosol.

	Original Transition Section Installed	New Transition Section Installed
Transport Tube Losses <sup>1</sup> (%)	1	3
Transition Section Losses <sup>2</sup> (%)	0	4
Impactor Stage Losses <sup>3</sup> (%)	17	18
Filter Top Assembly Losses <sup>4</sup> (%)	16	18
Impactor Efficiency <sup>5</sup> (%)	18	24
Filter Penetration <sup>6</sup> (%)	69	63

<sup>1</sup> Transport Tube Losses = transport tube mass / (mass collected on transport tube + transition section + impactor stage + impaction plate + filter assembly + afterfilter).

<sup>2</sup> Transition Section Losses = transition section mass / (mass collected on transition section + impactor stage + impaction plate + filter assembly + afterfilter).

<sup>3</sup> Impactor Stage Losses = impactor stage mass / (mass collected on impactor stage + impaction plate + filter assembly + afterfilter).

<sup>4</sup> Filter Top Assembly Losses = filter top assembly mass / (mass collected on filter top assembly + afterfilter mass).

<sup>5</sup> Impactor Efficiency = impactor plate mass / (mass collected on impactor plate + filter assembly + afterfilter).

<sup>6</sup> Filter Penetration = after filter mass / (mass collected on impactor plate + filter assembly + afterfilter).

Table 14. RAAMP sampler wash test results for 10 µm aerosol at 2 and 24 Km/hr with angled impactor stage and rectangular inlet installed (inlet separated from body).

Sampler Component	2 Km/hr		24 Km/hr	
	Uranine Conc µg/m <sup>3</sup>	Percent of Mass %	Uranine Conc µg/m <sup>3</sup>	Percent of Mass %
Cap	0.004	0	0.023	12
Deflector	0.002	0	0.016	8
Transport Tube	0.001	0	0.021	11
Transition	0.000	0	0.002	1
Impactor Stage	0.143	10	0.032	16
Impactor Plate	0.154	10	0.046	23
Filter Assembly Top	0.225	15	0.026	13
Afterfilter	0.976	65	0.033	16
Sum =	1.505		0.199	
Tunnel Concentration <sup>1</sup>	1.571		0.189	
Aspiration Efficiency <sup>2</sup>	96%		105%	
Percent Effectiveness <sup>3</sup>	62%		16%	

<sup>1</sup> Tunnel Conc determined using the isokinetic high volume ISO sampler.

<sup>2</sup> Aspiration Efficiency = total sampler collected mass concentration (Sum) divided by the Tunnel Conc.

<sup>3</sup> Percent Effectiveness = Afterfilter mass concentration divided by the Tunnel Conc.

**Table 15.** Particle transport losses attributed to individual components and characteristics of size fractionation components of the RAAMP sampler with the angled impactor stage and rectangular inlet installed for 10 µm aerosol at a wind speed of 2 km/hr and 24 Km/hr.

	2 Km/hr	24 Km/hr
Transport Tube Losses <sup>1</sup> (%)	0	13
Transition Section Losses <sup>2</sup> (%)	0	0
Impactor Stage Losses <sup>3</sup> (%)	10	23
Filter Top Assembly Losses <sup>4</sup> (%)	19	45
Impactor Efficiency <sup>5</sup> (%)	11	44
Filter Penetration <sup>6</sup> (%)	72	31

<sup>1</sup> Transport Tube Losses = transport tube mass / (mass collected on transport tube + transition section + impactor stage + impaction plate + filter assembly + afterfilter).

<sup>2</sup> Transition Section Losses = transition section mass / (mass collected on transition section + impactor stage + impaction plate + filter assembly + afterfilter).

<sup>3</sup> Impactor Stage Losses = impactor stage mass / (mass collected on impactor stage + impaction plate + filter assembly + afterfilter).

<sup>4</sup> Filter Top Assembly Losses = filter top assembly mass / (mass collected on filter top assembly + afterfilter mass).

<sup>5</sup> Impactor Efficiency = impactor plate mass / (mass collected on impactor plate + filter assembly + afterfilter).

<sup>6</sup> Filter Penetration = after filter mass / (mass collected on impactor plate + filter assembly + afterfilter).

Table 16. RAAMP sampler wash test results for 10 µm aerosol at 24 Km/hr with angled impactor stage and rectangular inlet installed (deflector removed and inlet separated from body).

Sampler Component	24 Km/hr	
	Uranine Conc µg/m <sup>3</sup>	Percent of Mass %
Cap	0.019	18
Deflector	NA	NA
Transport Tube	0.009	8
Transition	0.001	1
Impactor Stage	0.019	18
Impactor Plate	0.023	21
Filter Assembly Top	0.019	18
Afterfilter	0.018	17
Sum =	0.108	
Tunnel Concentration <sup>1</sup>	0.192	
Aspiration Efficiency <sup>2</sup>	56%	
Percent Effectiveness <sup>3</sup>	9%	

<sup>1</sup> Tunnel Conc determined using the isokinetic high volume ISO sampler.

<sup>2</sup> Aspiration Efficiency = total sampler collected mass concentration (Sum) divided by the Tunnel Conc.

<sup>3</sup> Percent Effectiveness = Afterfilter mass concentration divided by the Tunnel Conc.

**Table 17.** Particle transport losses attributed to individual components and characteristics of size fractionation components of the RAAMP sampler with the angled impactor stage and rectangular inlet installed for 10 µm aerosol at a wind speed of 24 Km/hr with the deflector removed from the inlet.

	24 Km/hr
Transport Tube Losses <sup>1</sup> (%)	10
Transition Section Losses <sup>2</sup> (%)	1
Impactor Stage Losses <sup>3</sup> (%)	24
Impactor Efficiency <sup>5</sup> (%)	38
Filter Penetration <sup>6</sup> (%)	30

<sup>1</sup> Transport Tube Losses = transport tube mass / (mass collected on transport tube + transition section + impactor stage + impaction plate + filter assembly + afterfilter).

<sup>2</sup> Transition Section Losses = transition section mass / (mass collected on transition section + impactor stage + impaction plate + filter assembly + afterfilter).

<sup>3</sup> Impactor Stage Losses = impactor stage mass / (mass collected on impactor stage + impaction plate + filter assembly + afterfilter).

<sup>4</sup> Filter Top Assembly Losses = filter top assembly mass / (mass collected on filter top assembly + afterfilter mass).

<sup>5</sup> Impactor Efficiency = impactor plate mass / (mass collected on impactor plate + filter assembly + afterfilter).

<sup>6</sup> Filter Penetration = after filter mass / (mass collected on impactor plate + filter assembly + afterfilter).

DUPCHECK-ID-NUMBER: 96001576907

PERMANENT-DOCUMENT-NUMBER: M96010070 000

<013>	DATE-COMPLETED	960525
<014>	DATE-OF-RECORD-ENTRY	960502
<015>	DATE-RECEIVED	960502
<016>	COPIES-RECEIVED	2
<020>	DOCUMENT-TYPE	R
<022>	MEDIUM-CODE	H
<030>	CLASSIFICATION-CODE	Uncl
<040>	LITERARY-INDICATOR	Y
<050>	GPO-SUPERINTENDENT-OF-DOCUMENTS	Y
<072>	PERSONAL-AUTHOR-AND-AFFILIATION	Vanderpool, R.W.; Peters, T.M.
<080>	SPONSORING-ORGANIZATION-CODE	DOE/EM
<110>	TITLE-ENGLISH	
	Wind tunnel evaluation of the RAAMP sampler. Final report	
<150>	PRIMARY-REPORT-NUMBER	DOE/RF/00646--T1
<240>	CONTRACT-NUMBER-DOE	AI34-93RF00646
<241>	ABBREV-CONTRACT-NUMBER-DOE	RF00646
<242>	AWARDING-OFFICE-CODE	34
<243>	BUDGET-REPORTING-CODE	?
<245>	LEGIBILITY-CODE	0
<246>	DOE-INITIATING-OFFICE-CODE	RF
<247>	MICROFICHE-DISTRIBUTION-CODE	4
<248>	VENDOR-ID-CODE	026670-0514-7
<249>	VENDOR-NAME	ENVIRONMENTAL PROTECTION AGCY
<251>	REPORTING-REQUIREMENT	?
<276>	DUPCHECK-BYPASS-FLAG	N
<291>	PACKED-PRIMARY-REPORT-NUMBER	DOERF00646T1
<293>	PREFIX	DE
<295>	INDEX-DOCUMENT-NUMBER	M96010070
<370>	PUBLICATION-DATE	Nov 1994
<376>	REPORT-TYPE-CODE-AND-FREQUENCY	F/93/96
<390>	PAGES-BIBLIOGRAPHIC	60
<400>	REPORT-DISTRIBUTION-CODE	A
<421>	LANGUAGE-CODE	EN
<425>	AUDIENCE-CODE	01
<426>	LIMITATION-CODE	UNL
<510>	DISTRIBUTION-CATEGORY	M -2000
<520>	PROJECT-STATUS	P
<530>	ANNOUNCEMENT-CODE	EDB;ERA;ETD;INS;NTS
<540>	EDB-SUBJECT-CATEGORIES	540130
<550>	SOURCE-OF-BIBLIOGRAPHIC-INPUT	IMS
<560>	COUNTRY-OF-INTELLECTUAL-ORIGIN	US
<570>	COUNTRY-OF-PUBLICATION	US
<600>	INIS-TYPE	R
<610>	INIS-CATEGORIES	B3310
<686>	DOCUMENT-STATUS-CODE	000
<700>	CORPORATE-CODE	9534824
<748>	TAPE-VOL-ISSUE	96R10
<749>	TAPE-INCOMING-SERIAL-NUMBER	AHC29610%%42
<801>	SUBJECT-DESCRIPTORS	
	PROGRESS REPORT;WIND TUNNELS;RADIOACTIVE AEROSOLS:T1;SAMPLING:Q1;AIR	
	SAMPLERS:T2;PERFORMANCE:Q2	
<805>	INIS-DESCRIPTORS	
	AIR SAMPLERS:T2;PERFORMANCE:Q2;PROGRESS REPORT;RADIOACTIVE AEROSOLS:T1;	
	SAMPLING:Q1;WIND TUNNELS	
<931>	AVAILABILITY-CODE	OS;NT;IN

DUPCHECK-ID-NUMBER: 96001576907

PERMANENT-DOCUMENT-NUMBER: M96010070 000

## &lt;950&gt; ABSTRACT

Wind tunnel tests of the Department of Energy RAAMP (Radioactive Atmospheric Aerosol Monitoring Program) monitor have been conducted at wind speeds of 2 km/hr and 24 km/hr. The RAAMP sampler was developed based on three specific performance objectives: (1) meet EPA PM10 performance criteria, (2) representatively sample and retain particles larger than 10 {micro}m for later isotopic analysis, (3) be capable of continuous, unattended operation for time periods up to 2 months. In this first phase of the evaluation, wind tunnel tests were performed to evaluate the sampler as a potential candidate for EPA PM10 reference or equivalency status. As an integral part of the project, the EPA wind tunnel facility was fully characterized at wind speeds of 2 km/hr and 24 km/hr in conjunction with liquid test aerosols of 10 {micro}m aerodynamic diameter. Results showed that the facility and its operating protocols met or exceeded all 40 CFR Part 53 acceptance criteria regarding PM10 size-selective performance evaluation. Analytical procedures for quantitation of collected mass deposits also met 40 CFR Part 53 criteria. Modifications were made to the tunnel's test section to accommodate the large dimensions of the RAAMP sampler's instrument case.